Earth's Future

RESEARCH ARTICLE
10.1029/2024EF004845

Global Assessment of Compound Climate Extremes and Exposures of Population, Agriculture, and Forest Lands Under Two Climate Scenarios

Tayler A. Schillerberg[1,2] and Di Tian[1]

[1]Department of Crop, Soil, and Environmental Sciences, Auburn University, Auburn, AL, USA, [2]USDA Midwest Climate Hub, Ames, IA, USA

Key Points:

- Global compound flash drought, heat wave, and extreme precipitation are projected to increase by the end of the century
- There are significant model agreements of compound heatwave and flash drought events compared to the other compound events
- Exposures of populations, agriculture, and forestry lands to sequential heatwaves and flash droughts show the largest increases

Supporting Information:

Supporting Information may be found in the online version of this article.

Correspondence to:

D. Tian,
tiandi@auburn.edu

Citation:

Schillerberg, T. A., & Tian, D. (2024). Global assessment of compound climate extremes and exposures of population, agriculture, and forest lands under two climate scenarios. *Earth's Future*, *12*, e2024EF004845. https://doi.org/10.1029/2024EF004845

Received 30 APR 2024
Accepted 16 AUG 2024

Abstract Climate change is expected to increase the global occurrence and intensity of heatwaves, extreme precipitation, and flash droughts. However, it is not well understood how the compound heatwave, extreme precipitation, and flash drought events will likely change, and how global population, agriculture, and forest will likely be exposed to these compound events under future climate change scenarios. This research uses eight CMIP6 climate models to assess the current and future global compound climate extreme events, as well as population, agriculture, and forestry exposures to these events, under two climate scenarios, Shared Socioeconomic Pathways (SSP), SSP1-2.6 and SSP5-8.5 for three time periods: early-, mid-, and late- 21st century. Climate extremes are derived for heatwaves, extreme precipitation, and flash droughts using locational-dependent thresholds. We find that compound heatwaves and flash drought events result in the largest increases in exposure of populations, agriculture, and forest lands, under SSP5-8.5 late-century projections of sequential heatwaves and flash droughts. Late-century projections of sequential heatwaves and flash droughts show hot spots of exposure increases in population exposure greater than 50 million person-events in China, India, and Europe; increases in agriculture land exposures greater than 90 thousand km^2-events in China, South America, and Oceania; and increase in forest land exposure greater than 120 thousand km^2-events in Oceania and South America regions when compared to the historical period. The findings from this study can be potentially useful for informing global climate adaptations.

Plain Language Summary There is lacking an understanding of how the compound heatwave, extreme precipitation, and flash drought events will likely change, and how global population, agriculture, and forest will likely be exposed to these compound events under future climate change scenarios. This paper presents a comprehensive assessment of the current and future global compound climate extreme events and population, agriculture, and forestry exposures to these events under two climate scenarios. We find that compound heatwaves and flash drought events have the largest increases in exposure of populations, agriculture, and forest lands, under a high emission scenario for late-century projections of sequential heatwaves and flash droughts. The results revealed hot spot regions of exposure to sequential heatwaves and flash droughts and consistent increases in population, agriculture, and forest land exposures for late-century projections. The findings from this study can potentially be useful for informing global climate adaptations.

1. Introduction

The World Economic Forum (2024) states that extreme weather events remained one of the top global concerns (extreme weather events, critical changes to Earth systems, biodiversity loss, ecosystem collapse, and natural resource shortages were ranked 1–4 on the list). The United States experienced 28 billion-dollar events totaling an estimated damage loss of 92.9 billion US dollars and 492 deaths, the National Centers for Environmental Information (NCEI) (2024) reported. These extreme events, such as heatwaves, extreme precipitation, and drought, experienced globally are becoming more common and projected to increase in future climate (Chen & Sun, 2015; Perkins-Kirkpatrick & Gibson, 2017; Ruosteenoja et al., 2018; Yuan et al., 2023). For example, heatwaves disrupt the thermoregulatory systems of humans and animals, leading to death (Gasparrini et al., 2015; Robinson, 2001), agriculture and ecosystems face reduced productivity as photosynthesis decreases (Alexandrov & Hoogenboom, 2000; Asseng et al., 2015; Peltonen-Sainio et al., 2011). Extreme precipitation resulting in floods is one of the deadliest events to humans (Ashley & Ashley, 2008), and standing flood waters can carry water-borne diseases (Charron et al., 2010). Delayed planting due to wet fields (Wolfe et al., 2018) and photosynthesis

decreases during the growing season from prolonged exposure to water can reduce yields (Mangani et al., 2018). Droughts can result in shortages of drinking water (Haile et al., 2020), increases in favorable wildfire conditions (Otkin et al., 2018), decreases in crop yield (Otkin et al., 2018), increases in livestock mortality (Nguyen et al., 2019), and increases tree mortality (Chitra-Tarak et al., 2018). Understanding the exposures to these extreme events is the prerequisite to making impactful climate adaptation strategies.

Extreme climate events are commonly analyzed as univariate extreme events. However, due to the interaction between compound events, their impacts may be underestimated (AghaKouchak et al., 2014; Fischer & Knutti, 2012). Here, we refer to the definition of compound events described by Zscheischler et al. (2018), where compound events are the combination of multiple drivers that contribute to societal or environmental risk; these drivers can span multiple spatial and temporal scales. There are four categories of compound events: pre-conditioned, multivariate, temporally compounding, and spatially compounding compound events (Zscheischler et al., 2020). Multiple studies (Mukherjee & Mishra, 2020; Wang et al., 2023; Zhou et al., 2023; Zscheischler et al., 2020) and the IPCC (Seneviratne et al., 2021) have concluded that compound events have increased at various rates around the globe. For example, current literature has largely focused on simultaneous hot-dry events which have increased from the recent historical past to the present (Feng et al., 2020; Wang et al., 2023) and future projected increases are more prominent when the RCP 8.5 scenario is considered (B. Liu et al., 2021; X. Wu et al., 2021; Yin et al., 2023; Y. Zhang et al., 2022; Zhou et al., 2023). Unfortunately, these compound events studies commonly use monthly (Das et al., 2022; Feng et al., 2020; X. Wu et al., 2021) or weekly (Mukherjee & Mishra, 2020; Ullah et al., 2023) drought and aggregate maximum temperatures to the same temporal scale despite their impacts can be on a smaller time scale, such as daily. Studies by Li et al. (2023) and Mukherjee and Mishra (2020) have tried to reduce this temporal scale limitation by observing drought as a monthly variable and heatwaves as a daily variable. This method, however, only allows simultaneous hot-dry events to be analyzed because of the temporal resolution mismatch, leaving sequential hot-dry events under-analyzed.

More recently, flash drought, characterized by its rapid development, is being explored at weekly or pentad scales and showing faster onset in a warming climate (Yuan et al., 2023). Flash droughts are a rapid onset of drought that can be measured on sub-seasonal time scales and triggered by increased evaporative demand or anomalously low precipitation (Hoffmann et al., 2021). Flash droughts causing rapid decreases in soil moisture can stunt crop growth and even result in crop failure (Otkin et al., 2018; Svoboda et al., 2002), increase livestock mortality (Nguyen et al., 2019), and cause quick changes in ecosystems that organisms and plants are unable to keep pace with (Otkin et al., 2016; M. Zhang & Yuan, 2020). Global projections by Yuan et al. (2023) and Christian et al. (2023) indicate that flash droughts will occur with higher frequency in future climates, and droughts may shift favorably to rapid flash droughts and away from gradual longer onset droughts. However, despite recent flash drought events like Russia in 2010 (Christian et al., 2020), Great Plains United States in 2012 (Otkin et al., 2016), northern High Plains United States in 2017 (Gerken et al., 2018), and Queensland, Australia in 2018 (Otkin et al., 2018), exposures to flash droughts and their compound events have not been well understood. Flash droughts triggered by heatwaves or heatwaves triggered by flash droughts can increase the risk to humans, agriculture, and ecology. The other sequential compound event of interest is flash droughts followed by heavy precipitation, which increases erosion and nutrient loading, potentially harming drinking water supplies for populations (Qiu et al., 2021). The rapid onset and impacts of flash droughts underscore the urgent need for proactive measures in water resource management and agriculture planning to mitigate their effects on ecosystems, agriculture, and communities, which requires the understanding of changes in exposures to flash droughts and their compound events.

Global studies of exposure to compound events beyond heatwaves and droughts are currently missing. Exposure has largely focused on population exposure to extreme temperatures (Jones et al., 2015; Keellings & Waylen, 2014; Lan et al., 2012). Or how warming temperatures affect agriculture yields (Krishnamurthy R et al., 2022; Ma & Yuan, 2021; Takle & Gutowski, 2020), which modifies the precipitation received, raising concerns about crop failure and food security (Krishnamurthy et al., 2022; Schillerberg & Tian, 2023). Regional studies (Das et al., 2022; Ullah et al., 2023) focus on areas with high populations, such as South Asia and China, and find an increase in exposure to these events with a continual increase in exposure in future climates. Global studies of population exposure to simultaneous hot-dry events also find an increase of up to 10-fold in some regions (Yin et al., 2023), with impacts being felt by 8.12 billion people a year as soon as mid-twenty-first century (Li et al., 2023). One study by Weber et al. (2020) analyzed exposure to current and future populations in Africa using multiple compound events. Where the cases of sequential and compound events were derived monthly.

Historically, the exposure of agriculture to compound hot-dry events has increased globally between 1950 and 2009 (Lesk & Anderson, 2021). Garry et al. (2021) showed an increase in exposure of UK agriculture to hot-wet compound events from current to future climates. Only a few studies focus on single drivers of forest exposure. Aleixo et al. (2019) and Anderegg et al. (2020) find that tree mortality is driven by direct climate impacts such as droughts, heatwaves, and flooding, which can increase tree mortality for up to 2 years after the climate event. Increased temperatures also draw into the question of whether forests remain carbon sinks or become carbon sources (Anderegg et al., 2020) in a changing climate. While existing research has provided valuable insights into the exposure of populations and agriculture to individual climate extremes, there remains a critical gap in understanding compound events beyond heatwaves and droughts.

To address these research gaps, this study aims to assess the projected changes of compound climate extremes: heatwaves, extreme precipitation, and flash droughts, and exposures of population, agriculture, and forestry to these events under two different Shared Socioeconomic Pathways (SSP) (O'Neill et al., 2014) (SSP1-2.6 and SSP5-8.5) over global land. We focus on multivariate compound events, where multiple events co-occur, and temporally compounding events, where an event occurs following a previous event. Efforts to comprehensively assess the impacts of simultaneous hot-dry events and other compound phenomena are essential for informing effective adaptation strategies and safeguarding global food security and ecosystem resilience in the face of a changing climate.

2. Materials and Methods

2.1. Climate Data

Daily data of maximum temperature (tasmax), precipitation (pr), and surface soil moisture (mrsos) were retrieved from eight CMIP6 models (Eyring et al., 2016), CMCC-ESM2, EC-Earth3, GFDL-ESM4, INM-CM4-8, INM-CM5-0, MPI-ESM1-2-HR, MRI-ESM2-0, NorSM2-MM detailed information is listed in Table S1 in Supporting Information S1. ERA5 (Hersbach et al., 2023) is used for an observational comparison of the historical period using the Root Mean Square Error and bias (see Text S1 and Table S2 in Supporting Information S1). Each model has a nominal resolution of 100 km for the period 1981–2100, where 1981–2010 is the historical period and 2011–2100 is the future period divided into early- mid- and late-century of equal lengths. Two future SSPs (O'Neill et al., 2014) were considered for 2015 onwards. SSP1-2.6, a sustainable route with 2.6 W/m^2 of relative forcing before 2100, is described as a peak and decline scenario. The second, SSP5-8.5, is described as fossil-fuel development having 8.5 W/m^2 of relative forcing before 2100 and presents societal challenges. These two scenarios present various plausible results that future societies may experience. All model data was bilinearly interpolated to $1° \times 1°$ resolution, and a mask compiled from available land data (limited by mrsos) was applied to all models to ensure compatible results.

2.2. Population and Land Use Land Change Data

We retrieved historical and future estimates to estimate global population, agriculture, and forest exposure to compound events. Historical population data for the reference period is available at a 1 km resolution from the Center for International Earth Science Information Network—CIESIN—Columbia University (2011, 2017), and De Sherbinin et al. (2012) for 1970–2000 decadal. Since the reference is only available to 2000, we use data from 1980 to 2000 to compute the historical average. Future populations for early-, mid-, and late-century were derived from Jones and O'Neil (2016, 2020), for both scenarios, which were originally available at 1/8th degree resolution. The population data sets were aggregated to $1° \times 1°$ resolution. It is important to note that future projections of populations may be biased; for example, the future China populations are biased as a result of recent fertility policy changes (Huang et al., 2019). Agriculture and forest land cover are available through land use harmonization (LUH2) (Hurtt et al., 2020; Popp et al., 2017). Which provides land use data from 850 to 2100 at $0.25° \times 0.25°$ yearly resolution using CMIP6 forcing data and results in historical and future data for SSP1-2.6 and SSP5-8.5 scenarios. The land use data was aggregated into $1° \times 1°$ resolution before combining land uses. Agriculture data is the cumulation of C3 (annual, nitrogen-fixing, and perennial) and C4 (annual and perennial) crops. Forest is the combined total fraction of primary and secondary forests. Since the land uses data is available as the fraction of the grid cell and grid cell area is influenced by latitude, spherical trigonometry (Karney, 2013) is used to calculate the area (km^2) of agriculture and forest in each grid cell, which is then used to calculate the exposure.

2.3. Methods

2.3.1. Climate Extremes

Three climate extremes are chosen to derive the compound events. The first climate extreme pertains to extremely warm temperatures lasting for extended periods, dubbed heatwaves. Heatwaves adversely affect populations, which may result in mortality, agriculture by decreasing yields, and ecosystems (Robinson, 2001). This study uses a location-dependent 95th percentile to account for the regional climate adaptation of populations and ecosystems. Xu et al. (2016) showed that using the 99th percentile may lead to an underestimation of mortality in human populations while a 90th percentile an overestimation of mortality. Heatwaves must last at least 3 days as this is when impacts on populations and ecosystems compound and become dire (Gasparrini et al., 2015; Lan et al., 2012; Robinson, 2001; Xu et al., 2016). Precipitation-derived extreme precipitation is the second climate extreme used in this study. Extreme precipitation may result in flooding events, the second most deadly climate extreme after heatwaves (Ashley & Ashley, 2008). Not only is extreme precipitation detrimental to populations via driving, drinking water contaminations, water-borne diseases, and the economy, but it can also affect aquatic and terrestrial ecosystems and agriculture (Charron et al., 2010; Tabari, 2020). For this study, extreme precipitation occurs when the 99th percentile, derived from wet days (days receiving more than 1 mm of precipitation), is exceeded. The third climate extreme is flash drought, a rapid onset of drought. Flash droughts have detrimental effects on agriculture (Otkin et al., 2018; Svoboda et al., 2002), livestock (Nguyen et al., 2019), and ecosystems (Otkin et al., 2018). Following Hoffmann et al. (2021), we define the occurrence of flash drought when the pentad of soil moisture in the top 10 cm declines from above the 40th percentile to the 10th percentile in 14 days or fewer, lasting at least 28 days before the soil moisture restores to above the 40th percentile. This definition differs from previous definitions of flash drought, which use root zone soil moisture and the 20th percentile (Ford & Labosier, 2017). Modifications implemented by Hoffmann et al. (2021) resulted from the data availability in the CMIP6 models and maintained similar event numbers.

2.3.2. Compound Events and Exposure

Zscheischler et al. (2018) define compound events as the combination of multiple drivers of hazards (i.e., heat, precipitation, wind) that contribute to increased risk in populations, agriculture, and ecosystems spanning multiple temporal and spatial scales. For this study, we focus on the climate extremes heatwave, extreme precipitation, and flash drought. Using the definitions in Zscheischler et al. (2020), we further explore simultaneous events, also called multivariate events, when two hazards occur at the same time and location. Moreover, sequential events or temporally compounding events occur when one hazard follows another in a given timeframe at the same location. Several compound climate extreme events were chosen for their relevancy and impacts. The compound climate extreme events we analyzed are:

- Simultaneous Heatwave and Flash Drought: A heatwave co-occurring with a flash drought.
- Sequential Heatwave and Flash Drought: A heatwave is followed by a flash drought within 7 days.
- Sequential Flash Drought and Heatwave: A flash drought is followed by a heatwave within 7 days.
- Sequential Flash Drought and Extreme Precipitation: A flash drought is followed by extreme precipitation within 7 days.

We analyze the change in exposure for population, agriculture land area, and forest land area individually for each grid cell. To calculate exposure for each grid cell, we multiply the population or land area by the number of occurrences of the compound events, following Mishra et al. (2017).

3. Results

3.1. Projected Changes in Heatwave, Extreme Precipitation, and Flash Drought

We calculate a baseline for future climate scenarios from the historical period to investigate the changes in individual climate extremes (Figure S1 in Supporting Information S1). Figure 1 shows the difference between the historical baseline and the late-century climate scenarios SSP1-2.6 and SSP5-8.5 for the climate extremes. Globally, we find an increase in heatwaves and extreme precipitation events. The SSP5-8.5 scenario projects the highest increase in heatwave events compared to the historical baseline and the SSP1-2.6 scenario. The largest increase of over 600 additional heatwave events occurs in western South America and the Oceania regions. Late-century SSP5-8.5 projections of these areas and central Africa show increases in extreme precipitation, with

10.1029/2024EF004845

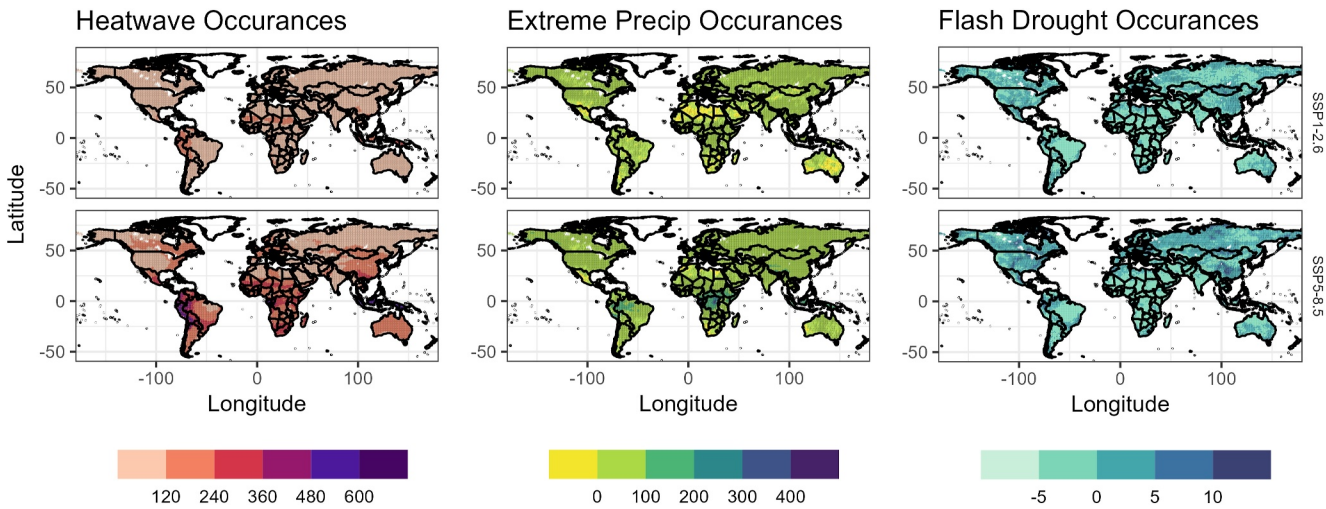

Figure 1. Projected change of occurrence for climate extremes. Late-century (2071–2100) differences with the historical period when compared to two different climates scenarios: SSP1-2.6 (top row) and SSP5-8.5 (bottom row) for heatwaves, extreme precipitation, and flash drought. High model agreement is when six or more models agree on the direction of change between future and historical occurrences. High model agreement areas are hashed.

portions of central Africa showing an additional 400 events. Figure 1 also shows the uncertainty and consistency of the direction of sign change (increase or decrease) of events, where high model agreement occurs when at least 6 of the 8 models agree on the direction of change between the historical and future time periods. Amongst the three events, the largest uncertainty (inconsistent change) occurs in mid-century (not shown) and in the SSP1-2.6 projections. Disagreement in the direction of change in late-century SSP1-2.6 extreme precipitation events occurs in Australia, northern and southern Africa, South America, portions of North America, and Asia (Figure 1) largely arid regions. There are large disagreements in flash drought occurrence where only small pockets of agreement exist in the SSP5-8.5 projections. The agreement areas coincide with areas where at least 10 additional flash drought events may occur late-century in central and eastern North America, China, western Europe, and western South America.

In Figure 2, we present a 10-year moving average of global grid cells experiencing high agreement in the change of climate extreme events. Our results show that during the historical period, on average, 74 heatwave events occurred globally (Figure S1 in Supporting Information S1), equaling 2.4 heatwave events in a given year (Figure 2). The number of heatwaves increases with time for both scenarios, with the highest number of events occurring mid- to late-century in SSP1-2.6 model projections (average 143 total events, 4.6 events per year) and late-century in the SSP5-8.5 scenario (average 224 total events, 7.2 events per year). Globally, on average, the historical period includes 40 extreme precipitation events (Figure S1 in Supporting Information S1), which is about 1.3 events per year (Figure 2). Figure 2 shows an increase in extreme precipitation events and model spread by late-century for SSP5-8.5 model projections, resulting in an average of 80 events during the period. In contrast, SSP1-2.6 displays a leveling of extreme precipitation events mid-century into late-century with a slight increase for an average of 52 events per period (1.7 events per year). Unlike heatwaves and extreme precipitation, flash drought events occur in smaller numbers with less change between the historical and future time periods (Figures 1 and 2). The historical period averages six events (0.2 events per year) globally (Figure S1 in Supporting Information S1), which increases to an average of seven events (for the late-century time period when SSP1-2.6 is considered and eight events for the SSP5-8.5 scenario (Figure 2)). Figure 2 shows overall flash droughts have shown little change with high variability in event occurrence.

In Figure 3, we further explore grid cells with consistent changes between the historical and future periods of extreme events. To do this, we construct joint frequency distributions. The scatterplots of paired climate extremes show a gradual increase in flash drought compared with heatwaves and flash droughts compared with extreme precipitation events in the SSP1-2.6 late-century scenario, while heatwaves paired with extreme precipitation have a larger increase between the early- and late-century time periods. Paired extreme events in the SSP5-8.5 scenario show a continual, distinct increase, represented by clustering, in the difference between events in the

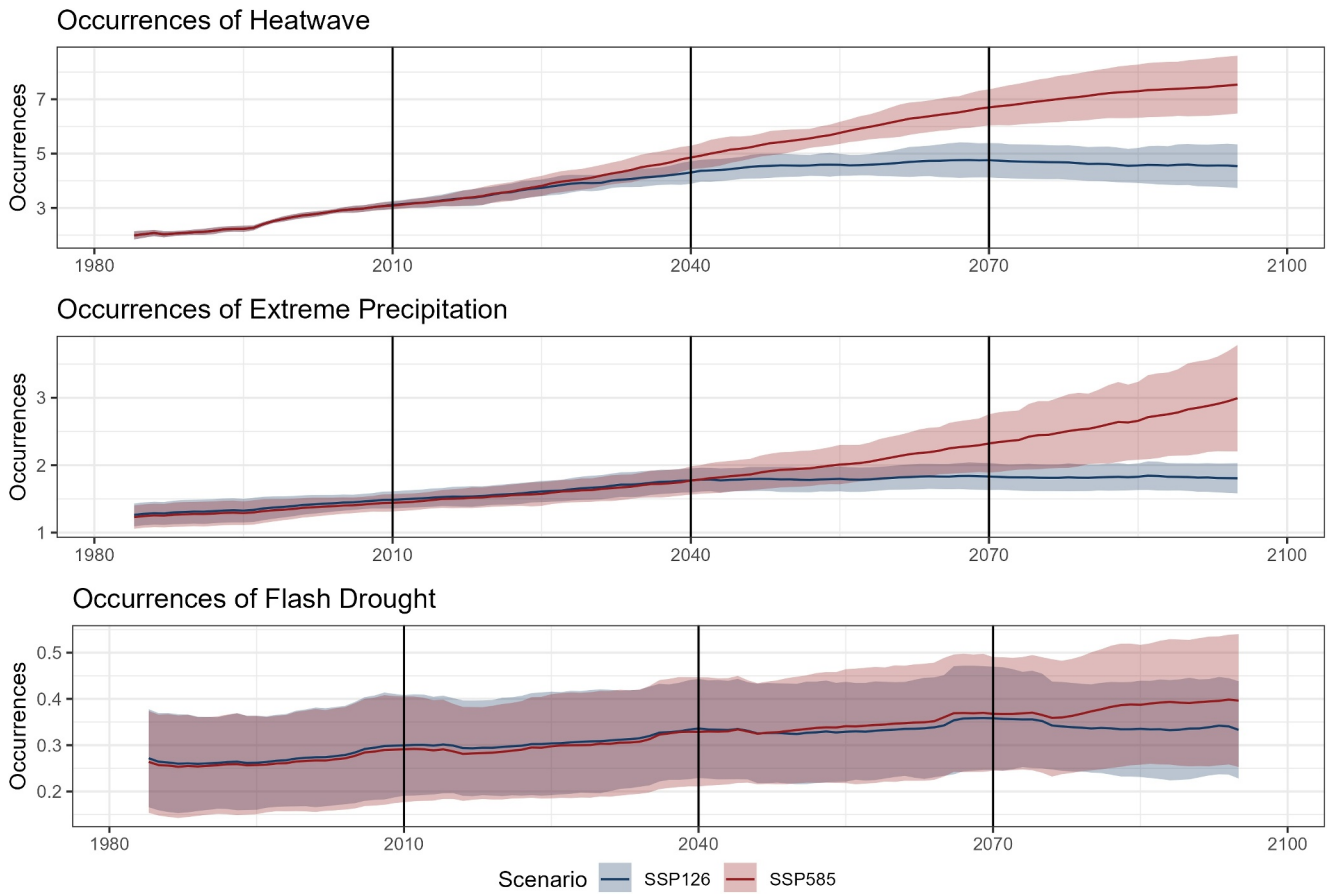

Figure 2. Using significant grid cells, historical and projected frequency of heatwave, extreme precipitation, and flash drought occurrences. Solid lines represent the 10-year moving average of the ensemble mean, and shaded areas represent one standard deviation of the ensemble mean. High model agreement is when six or more models agree on the direction of change between future and historical occurrences.

historical period and the early-, mid-, and late-century. Axis distributions also show this distinct clustering between time periods, which is more apparent in the SSP5-8.5 scenario than the SSP1-2.6 scenario.

3.2. Projected Changes in Compound Extreme Events

The regions of North America and China experienced a regional average of three simultaneous heatwave and flash drought occurrences during the historical period, while the rest of the globe averaged near zero events (Figure S2 in Supporting Information S1). This is likely due to the large uncertainty surrounding flash drought (Figure 2) due to soil moisture representation and inconsistent change (Figure 1). Late-century model projections of simultaneous heatwave and flash drought events for both the SSP1-2.6 and the SSP5-8.5 scenarios generally show inconsistent changes in the compound event (Figure 4). Again, this is likely due to the large uncertainty associated with changes in flash drought from the historical to future projections (Figure 2). Despite this, areas of agreement in the compound event changes exist in central North America, western South America, China, Mongolia, and Oceania under SSP5-8.5; however, the areas of agreement drastically reduce under the SSP1-2.6 scenario. Regions in northern South America and Oceania have consistent increases in simultaneous heatwave and flash drought occurrences, with an increase of over 10 events during the late-century SSP5-8.5 period. These regions and portions of China and North America coincide with consistent increases in flash drought occurrences when SSP5-8.5 late-century is considered (Figure 1).

Sequential heatwave and flash drought compound events occur more during the historical reference period than simultaneous heatwave and flash drought events. The historical period has a global average of 4.3 sequential heatwave and flash drought events, with local events exceeding 12 in North America and northern and central Asia regions (Figure S2 in Supporting Information S1). The SSP5-8.5 climate scenario projects an increase to

10.1029/2024EF004845

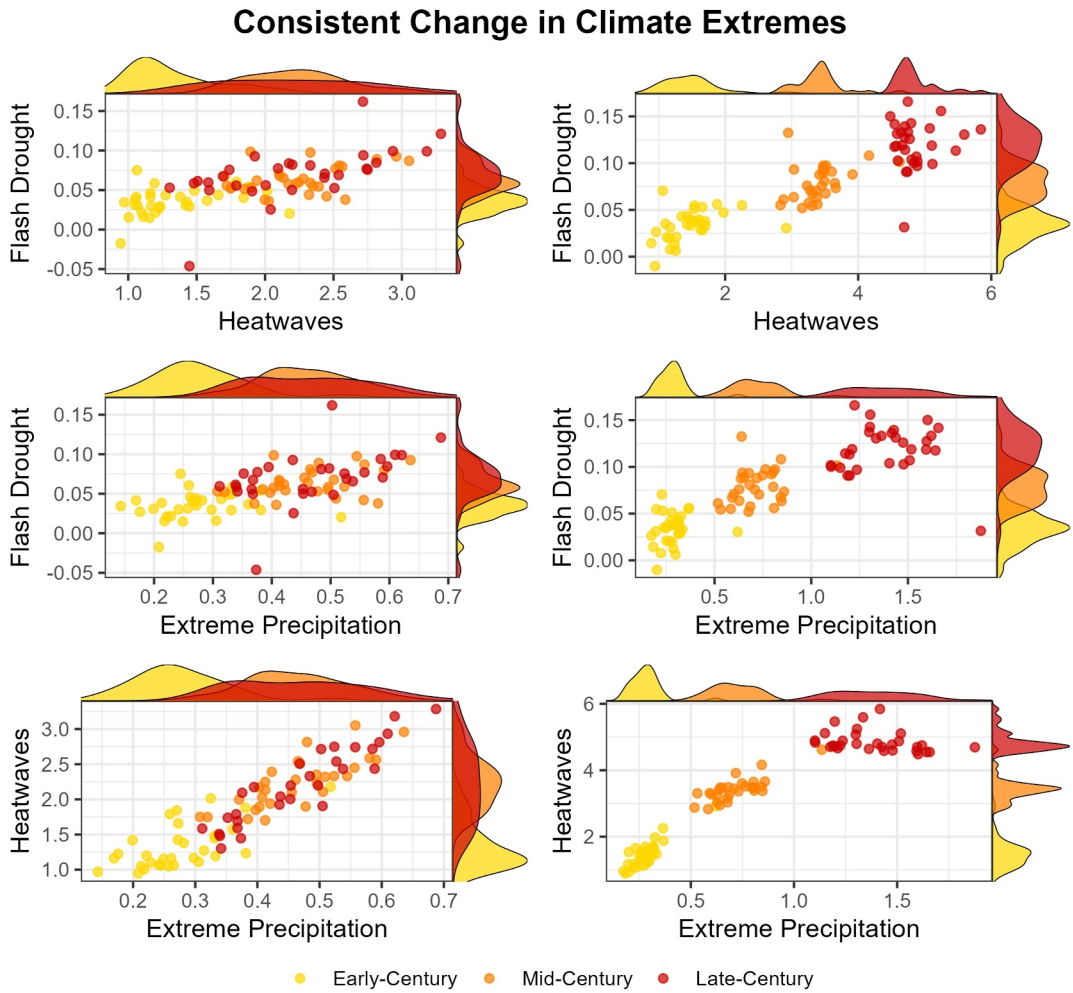

Figure 3. Joint frequency of climate extremes at locations experiencing consistent change. Distribution of changes in the annual occurrence frequency for heatwaves and flash droughts (top row), extreme precipitation and flash drought (middle row), and extreme precipitation and heatwaves (bottom row) for early- (yellow), mid- (orange), and late- (red) century using SSP1-2.6 (left column) and SSP5-8.5 (right column). High model agreement change occurs when six or more models agree on the direction of change between future and historical occurrences.

30+ sequential heatwave and flash drought events for the late-century period or roughly one event a year in some regions. Additionally, late-century SSP5-8.5 projections show regions of agreement in northern and central South America, southern Africa, Europe, and Australia with at least five additional sequential heatwave and flash drought events compared to the historical period. Again, the spatial pattern of late-century SSP5-8.5 occurrences of sequential heatwaves and flash drought resembles the projected flash drought occurrence change (Figure 1).

Throughout the historical period, sequential flash drought followed by heatwave events occurred minimally, ranging from 0 to 1.6 events across the globe, due to the rarity of the events and model representation (Figure S2 in Supporting Information S1). However, under SSP5-8.5 late-century projections, the occurrence increases 14 events in portions of South America and by five events in China, Oceania, and southern South America (Figure 4). Late-century SSP1-2.6 projections result in few occurrences and fewer occurrences, with fewer locations agreeing on the changes greater than two events (Figure 4). Overall, both the SSP1-2.6 and SSP5-8.5 scenarios show non-consistent changes in sequential flash drought and heatwave occurrences, except in the former mentioned regions of China, Oceania, and South America. Like the previously discussed simultaneous and sequential heatwave and flash drought compound events, late-century SSP5-8.5 spatial patterns of sequential heatwave and flash droughts are influenced by the spatial pattern of flash drought of the same period and scenario.

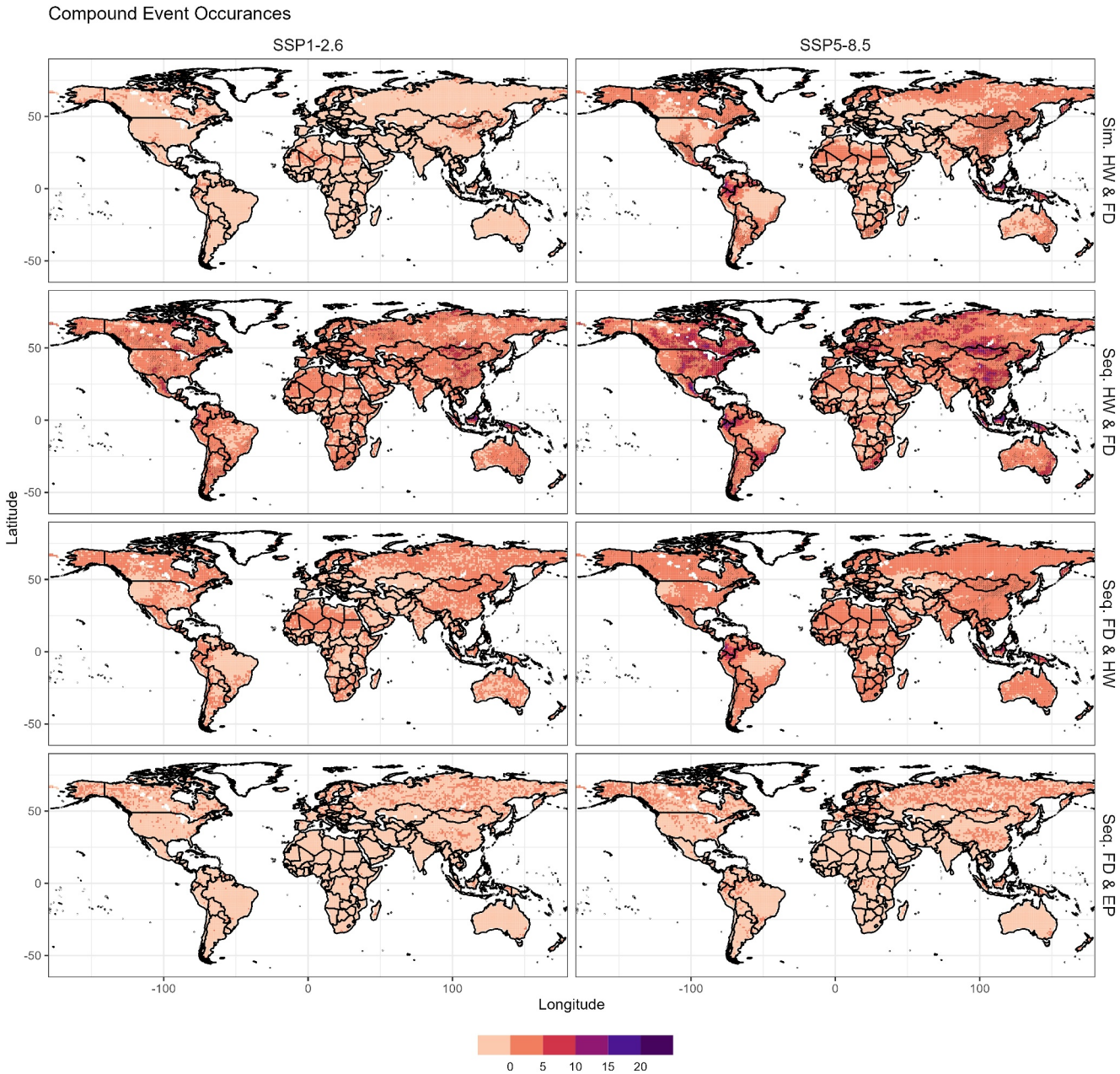

Figure 4. Change in compound events to future projection for SSP1-2.6 (left column) and SSP5-8.5 (right column) late-century from the historical baseline. Compound events from top to bottom: simultaneous heatwave and flash drought (Sim. HW and FD), sequential heatwave followed by flash droughts (Seq. HW and FD), sequential flash drought followed by heatwave (Seq. FD and HW), and sequential flash drought followed by extreme precipitation (Seq. FD and EP). High model agreement change occurs when six or more models agree on the direction of change between future and historical occurrences. High model agreement areas are hashed.

Sequential flash drought and extreme precipitation events in the historical period are near zero when averaged amongst the models (Figure S2 in Supporting Information S1). Both scenarios show inconsistent directional changes at all locations when sequential flash drought and extreme precipitation events are projected into the late-century (Figure 4). The projected inconsistent additional events largely occur in the upper latitudes (50°N) and in central China, with smaller pockets in Oceania, Central Africa (Democratic Republic of the Congo), South America, and the central United States. These locations coincide with some of the largest projected occurrence increases of extreme precipitation and flash drought in the late-century SSP5-8.5 scenario (Figure 1), increasing the likelihood of events occurring in the future.

Table 1
Selected Regions to Compute Exposure

Region	Population, agriculture, or forest changes	Extreme event changes	Compound event changes
Africa	Population, Agriculture, Forest	Heatwaves, Extreme Precipitation	–
China	Population, Forest	Heatwaves, Flash Drought	Seq. HW and FD
Europe	Population	Heatwaves	Seq. HW and FD
India	Population, Agriculture	–	
North America	Population, Agriculture	Heatwaves, Flash Drought	Seq. HW and FD
Oceania	–	Heatwaves, Extreme Precipitation	Sim. HW and FD, Seq. HW and FD, Seq. FD and HW
South America	Population, Agriculture, Forest	Heatwaves, Extreme Precipitation	Sim. HW and FD, Seq. HW and FD, Seq. FD and HW

Note. Each region was chosen due to consistent or large changes in population, agriculture or forest land area, extreme events, and compound events.

3.3. Projected Changes in Exposures to Compound Extreme Events

We further explore the exposure of populations, agriculture, and forest to compound extreme events. To do this, we combine the projected changes in population and land use with our compound event projections globally and highlight regional areas of consistent changes. The regions of interest come from the projections of compound events and regional hotspots of populations, agriculture, and forest (Table 1, Figure 5). Before each section and detailed regional analysis, we highlight the major changes in population, agriculture, and forest for each of the seven regions and a generalized overview of changes in compound event exposure.

3.3.1. Projected Exposures of Populations to Compound Climate Extremes

The most notable population changes in the regions selected include an overall decrease in populations in China and South America, which are present in both scenarios (Figure 5). Other regions, such as Africa, Europe, North America, and Oceania, have experienced more localized increases in populations. Globally, compound events derived from heatwaves and flash droughts show an increase in population exposure by the late-century under both SSP1-2.6 and SSP5-8.5 (Figure 6). Regions of decrease largely exist in the northern latitudes (northern North America and Russia) and portions of South America and Australia. However, only slight differences from zero are noted for population exposure to sequential flash drought and extreme precipitation.

Simultaneous heatwave and flash drought events occur in China, Europe, North America, Oceania, and South America, with an average exposure of 70,000 person-events during the historical period (Figure S3 in Supporting

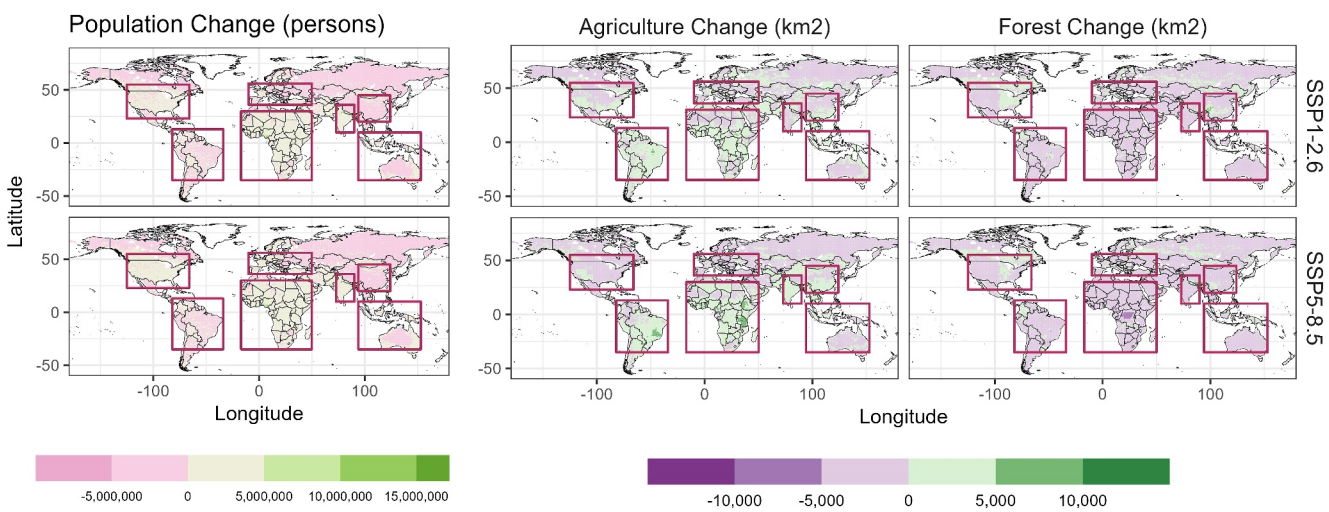

Figure 5. Projected differences of populations (first column), agriculture land use (middle column) and forest land use (right column). Differences are calculated using the historical period compared to two climate scenarios: SSP1-2.6 (top row) and SSP5-8.5 (bottom row). Bounded regions represent areas of interest; these areas are described in Table 1.

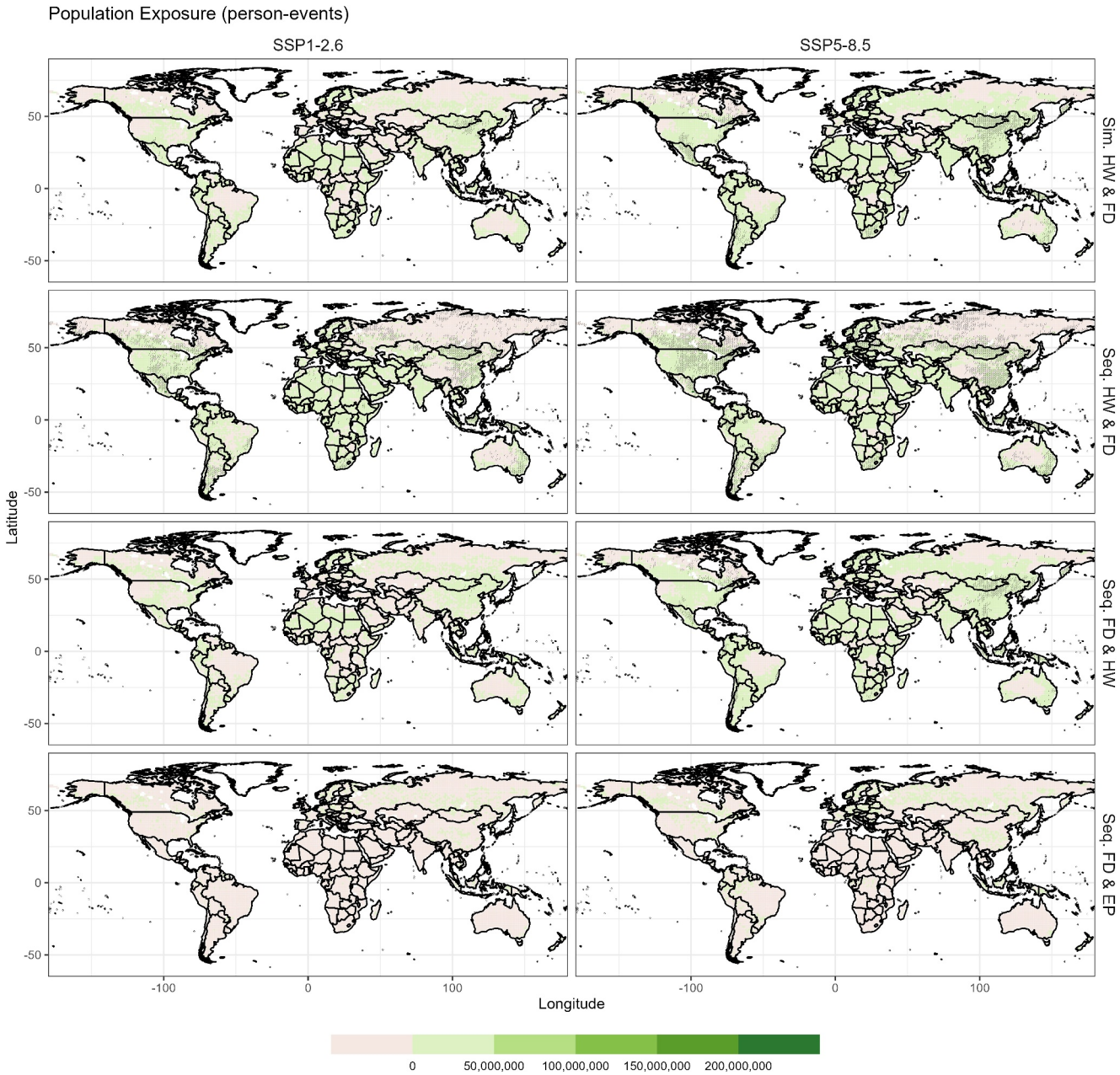

Figure 6. Change in population exposed to simultaneous heatwave and flash drought (Sim. HW and FD), sequential heatwave followed by flash drought (Seq. HW and FD), sequential flash drought followed by heatwave (Seq. FD and HW), and sequential flash drought followed by extreme precipitation (Seq. FD and EP) during early-, mid-, and late-century under SSP1-2.6 (left column) and SSP5-8.5 (right column) compared to historical. High model agreement areas are hashed.

Information S1). When considering late-century SSP1-2.6 (Figure 7) projections, changes in population exposure increase to an average of 194,000 person-events and 801,000 person-events in the SSP5-8.5 scenario (Figure 8). Regionally, China and India have the highest exposure increase, with an additional 1.5+ million person-events projected by late-century under the SSP5-8.5 scenario and fewer than 500,000 person-events in the SSP1-2.6 scenario. Decreases in projected population exposures in the SSP1-2.6 scenario in the regions of China and Oceania from mid- to late-century are likely due to the slower increases in extreme events (Figure 2) and population growth. The population exposure projected increased changes for Africa, Europe, North America, Oceania, and South America, which are less than 600,000 person-events under SSP5-8.5 and fewer than 100,000 person-events for the SSP1-2.6 scenario.

10.1029/2024EF004845

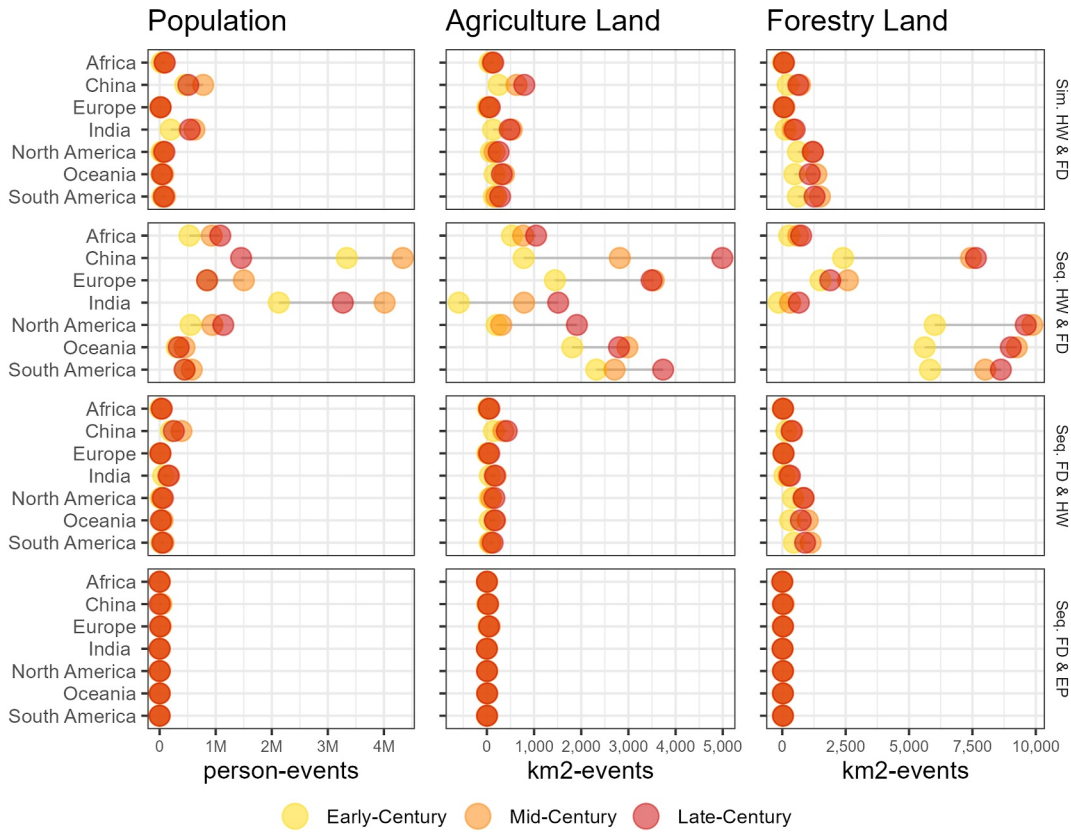

Figure 7. Change in population (left column), agriculture land area (middle column), and forest land area (right column) exposed to simultaneous heatwave and flash drought (Sim. HW and FD), sequential heatwaves followed by flash droughts (Seq. HW and FD), sequential flash droughts followed by heatwaves (Seq. FD and HW), and sequential flash droughts followed by extreme precipitation (Seq. FD and EP) during early-, mid-, and late-century under SSP1-2.6 compared to historical.

Throughout the historical period, sequential heatwave and flash drought events resulted in an average population exposure of 2.13 million person-events—the highest of the four compound events analyzed (Figure S3 in Supporting Information S1). This compound event also had the highest regional increased exposure for all events and scenarios. Late-century SSP5-8.5 and SSP1-2 scenarios project an average increase of 2.15 million person-events and 1.22 million person-events, respectively. Regionally, China, Europe (SSP1-2.6 only), India, Oceania, and South America have a higher increase in population exposure mid-century compared to late-century for both SSP5-8.5 and SSP1-2.6 scenarios. The highest population exposure is projected SSP5-8.5 for the China region mid-century with an additional 4.76 million person-events (Figure 8) compared to the historical period and decreases to an additional 2.61 million person-events compared to the reference period. The changes in China are likely due to over-estimated population decreases toward the end of the century and the lengthening of events (historical 31 days; SSP1-2.6 late-century 36 days; SSP5-8.5 late-century 43 days). Exposure is defined as event occurrence multiplied by the population for that time period. As a result, a lengthening of compound events may decrease the overall number of compound events experienced, artificially decreasing the population exposure, as fewer events may occur over the same period. The India region also experiences a decrease in exposure from the mid- to late-century, though this region did not have a large population decrease. In both scenarios, Oceania and South America have the smallest increase in population exposure with less than an additional 1 million person-events exposure. Projected changes in SSP1-2.6 suggest that exposure to sequential heatwave and flash drought events may decrease to early-century levels by late-century while remaining higher than the historical period in Europe, South America, and Oceania.

Sequential flash drought and heatwave events occur less frequently than the formally mentioned compound events. This results in a historical regional average exposure of 17,000 person-events (Figure S3 in Supporting

10.1029/2024EF004845

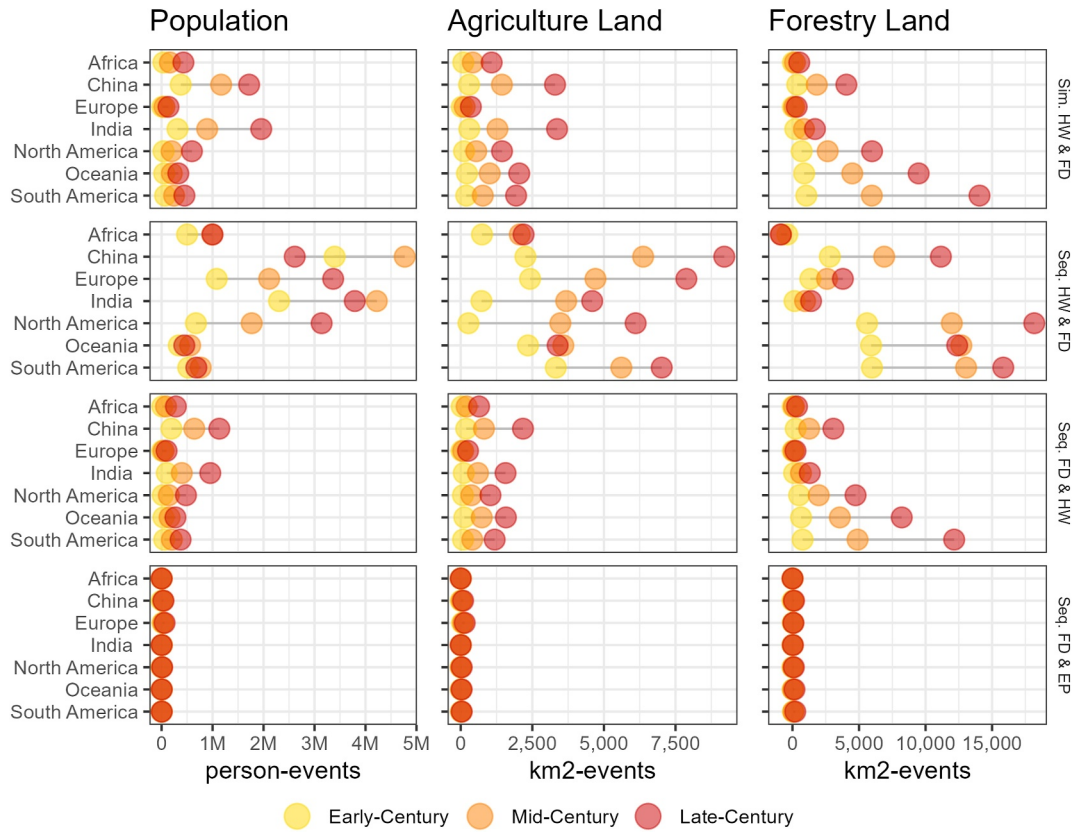

Figure 8. Change in population (left column), agriculture land area (middle column), and forest land area (right column) exposed to simultaneous heatwave and flash drought (Sim. HW and FD), sequential heatwaves followed by flash droughts (Seq. HW and FD), sequential flash droughts followed by heatwaves (Seq. FD and HW), and sequential flash droughts followed by extreme precipitation (Seq. FD and EP) during early-, mid-, and late-century under SSP5-8.5 compared to historical.

Information S1). SSP5-8.5 scenario projections for late-century regions of China and India show the highest increase in exposure, 1.13 million and 955,000 person-events (Figure 8), respectively. However, under the SSP1-2.6 scenario, the exposure is the highest for mid-century at 389,000 and 169,000 additional person-events, decreasing additional exposure to 253,000 and 158,000 person-events by late-century. Africa, Europe, North America, and South America are projected to increase under 500,000 person-events in SSP5-8.5 and less than 60,000 person-events under SSP1-2.6 scenarios.

The historical average for regional sequential flash drought and extreme precipitation is 5,100 person-events (Figure S3 in Supporting Information S1) and only shows marginal increases in SSP5-8.5 and SSP1-2.6 projections when compared to the other compound events. China and Europe SSP5-8.5 late-century projected exposure increases to an additional 35,000 and 58,800 person-events, respectively; smaller changes of 31,000 and 21,000 person-events are projected in SSP1-2.6 mid-century. North America is also projected to experience an increase in additional population exposure greater than 10,000 when SSP5-8.5 late-century is considered, but less than 5,000 additional person-events when SSP1-2.6 is considered. Africa, India, Oceania, and South America SSP5-8.5 also projects minor increases in additional population exposure; however, projections for India show a slight decrease of fewer than 340 person-events for SSP1-2.6 mid- and late-century.

3.3.2. Projected Exposure to Agricultural Lands to Compound Climate Extremes

Changes in agricultural area exposure are essential for understanding food security in future climates. Projected changes in agricultural areas vary across the chosen regions. In China and India, changes to agricultural areas occur in SSP5-8.5 projections, with less notable changes under SSP1-2.6 (Figure 5). There are some decreases in northern China, but sizable cropland areas are increasing in southern China and southern India. Europe has a small

projected decrease in agriculture areas in both scenarios. Agriculture area projections (both scenarios) in North America anticipate decreases in central North America, which is commonly considered a high-production region. SSP1-2.6 projects small increases along the East Coast. Both scenarios show little overall change in the agricultural area of Oceania. South America, especially Brazil, is projected to increase its agricultural area in SSP5-8.5 and, to a lesser degree, in SSP1-2.6. Africa's agricultural lands are projected to have small increases under SSP1-2.6 and larger increases and decreases under SSP5-8.5, with the largest increases occurring in East-central Africa. Simultaneous and sequential heatwave and flash drought events and, to a greater extent, sequential flash drought and heatwave events show decreases in agricultural land area exposed to compound events in northern latitudes of North America and Russia, portions of Africa, Australia, and north-east regions of South America. However, there are notable areas of increase in eastern Asia, islands in the Oceania region, southern Australia, India, Africa, southeastern South America, and central North America. These increases are less apparent in SSP1-2.6, resulting in decreases in agricultural exposure. Globally, agriculture exposure derived from sequential flash drought and extreme precipitation results in inconsistent changes, with overall decreases and the most prominent increases in exposure throughout China and North America.

The historical baseline of agriculture area exposure for the simultaneous heatwave and flash drought in the five regions is 150 km^2-event (Figure S4 in Supporting Information S1). The SSP5-8.5 and SSP1-2.6 scenarios project an increase of additional exposure of 2,000 km^2-event (Figure 8) and 330 km^2-event (Figure 7). China is a region that is projected to experience increases and decreases in agricultural land and has a high model agreement of increases in simultaneous heatwave and flash drought events (Figures 5 and 9). China and India are projected to have the highest additional agriculture exposure for both scenarios, with an additional exposure of 3,300 km^2-event (each) for SSP5-8.5 and 790 km^2-event 480 km^2-event for SSP1-2.6, respectively. Strong increases in the simultaneous heatwave and flash drought events and model agreement lead to an increase in exposure over 2,000 km^2-event for SSP5-8.5 projections. Projected changes in Africa, Europe, and North America remain below 1,500 km^2-event for SSP5-8.5 late-century and below 300 km^2-event for Africa, Europe, North America, Oceania, and South America under SSP1-2.6. Historically, agriculture exposure to sequential heatwave and flash drought events has been 5,700 km^2-event for the selected regions (Figure S4 in Supporting Information S1). However, future scenarios project substantial increases in additional agricultural exposure from sequential heatwave and flash drought events compared to the other compound events. By late-century, the SSP5-8.5 scenario results in an additional 5,700 km^2-events and 2,800 km^2-events of agriculture exposure in SSP1-2.6. China, Europe, North America, and Oceania all have high model agreement in the SSP5-8.5 scenario and show increases in agriculture exposure (Figure 9). The model agreement in Africa and South America is sparse, with smaller increases in agricultural exposure. Compared to the SSP1-2.6 scenario, there is less model agreement and smaller increases in agricultural exposure. China is projected to have the largest increases in agriculture exposure of 8,200 km^2-event and 5,000 km^2-event late-century followed by Europe and South America.

Sequential flash droughts and heatwaves have a historical agriculture exposure of 40 km^2-event (Figure S4 in Supporting Information S1). Only regionally in China is the historical agriculture exposure higher than 100 km^2-events, increasing to an additional 2,100 km^2-event and 400 km^2-event by late-century projects the SSP5-8.5 and SSP1-2.6 scenarios. India and the Oceania region have the highest projected increases in agriculture exposure of nearly 1,500 km^2-event by late-century in the SSP5-8.5 scenario, remaining below 200 km^2-event in the SSP1-2.6 scenario. Africa, Europe, North America, and South America agriculture exposure increases less than 1,200 km^2-event in the SSP5-8.5 scenario and less than 100 km^2-event in the SSP1-2.6 scenario.

Agriculture exposure to sequential flash droughts and extreme precipitation is historically 12 km^2-event (Figure S4 in Supporting Information S1) for the regions and remains very small with projected increases of 2–140 km^2-event for the SSP5-8.5 scenario and 2–60 km^2-event for the SSP1-2.6 scenario. The projected inconsistency of change direction (increase or decrease) of sequential flash drought and extreme precipitation compound events even by late-century (Figure 4) is likely contributing to minute changes in agriculture exposure.

3.3.3. Projected Exposure of Future Forest Lands to Compound Climate Extremes

Large spatial changes in global forests can impact the global carbon budget and influence CO_2 in the atmosphere (Anderegg et al., 2020). Notable changes in the analyzed regions include overall projected decreases in all regions (Figure 5), with the largest decrease in forest area occurring in southern central Africa. There are small areas of increase in forest area in southern China for both scenarios and northern China, mainly in SSP1-2.6. SSP1-2.6

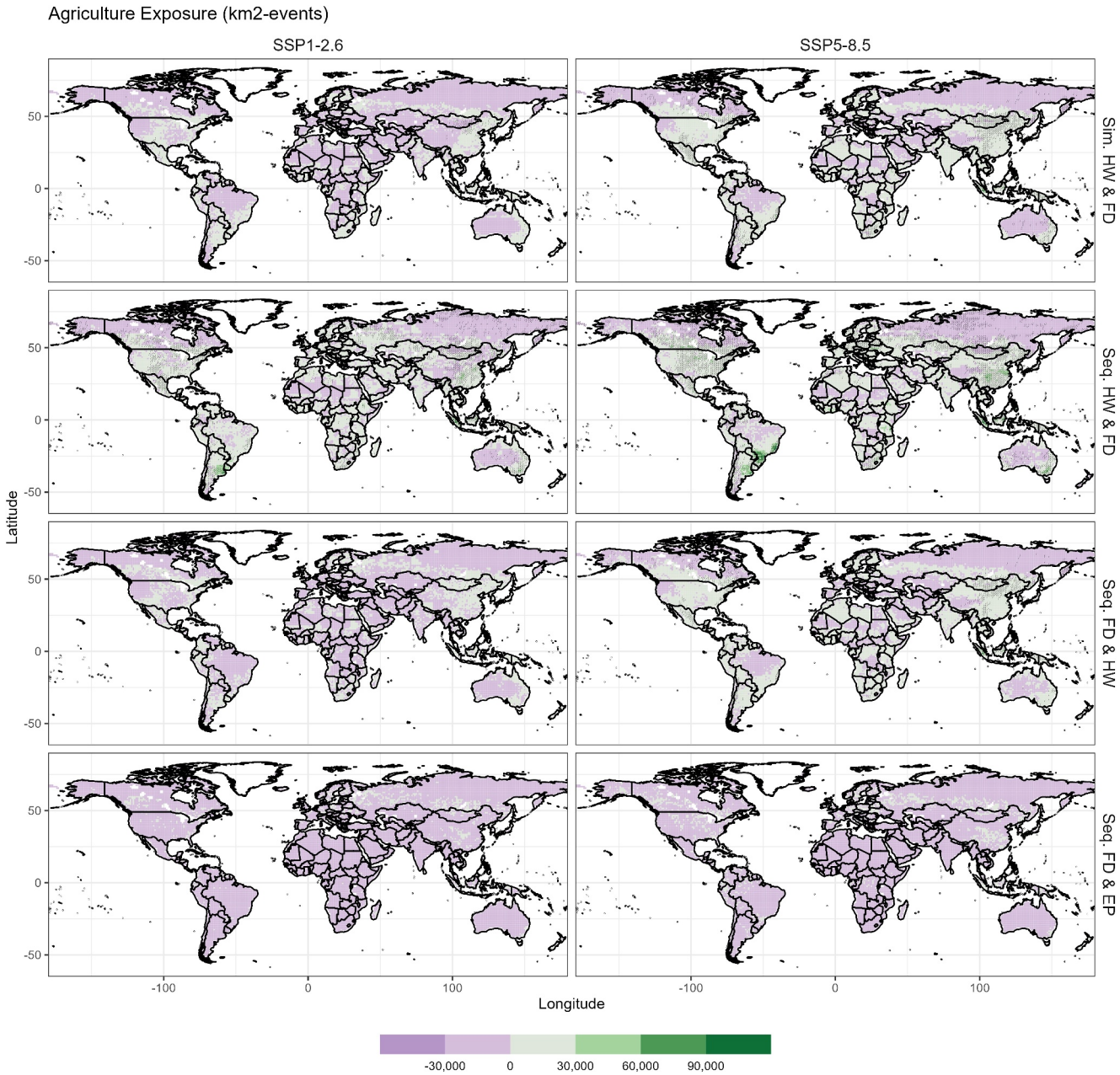

Figure 9. Change in agriculture land area exposed to simultaneous heatwave and flash drought (Sim. HW and FD), sequential heatwaves followed by flash droughts (Seq. HW and FD), sequential flash droughts followed by heatwaves (Seq. FD and HW), and sequential flash droughts followed by extreme precipitation (Seq. FD and EP) during early-, mid-, and late-century under SSP1-2.6 (left column) and SSP5-8.5 (right column) compared to historical. High model agreement areas are hashed.

scenarios project minute increases in European forest areas. Under SSP5-8.5, North America is projected to have increases in forest areas east of 100° W and increases in forest areas where crop production has been more dominant in the past. The Oceania region largely experiences small decreases in forest areas for both scenarios. Northern South America is projected to have increases in forest area under SSP1-2.6 and to a minor degree in SSP5-8.5. Globally, all four compound events show similar regional increases in forest land area (Figure 10). There is an increase of exposure in southern China, across Russia into Europe, and the islands that make up the Oceania region, central Africa, northern South America, and northern and eastern North America. Meanwhile, areas not mentioned experience decreases in forest land area exposure. Sequential flash drought and extreme precipitation show the largest areas of potential decreases in exposure; however, these changes are uncertain because of vast model disagreement.

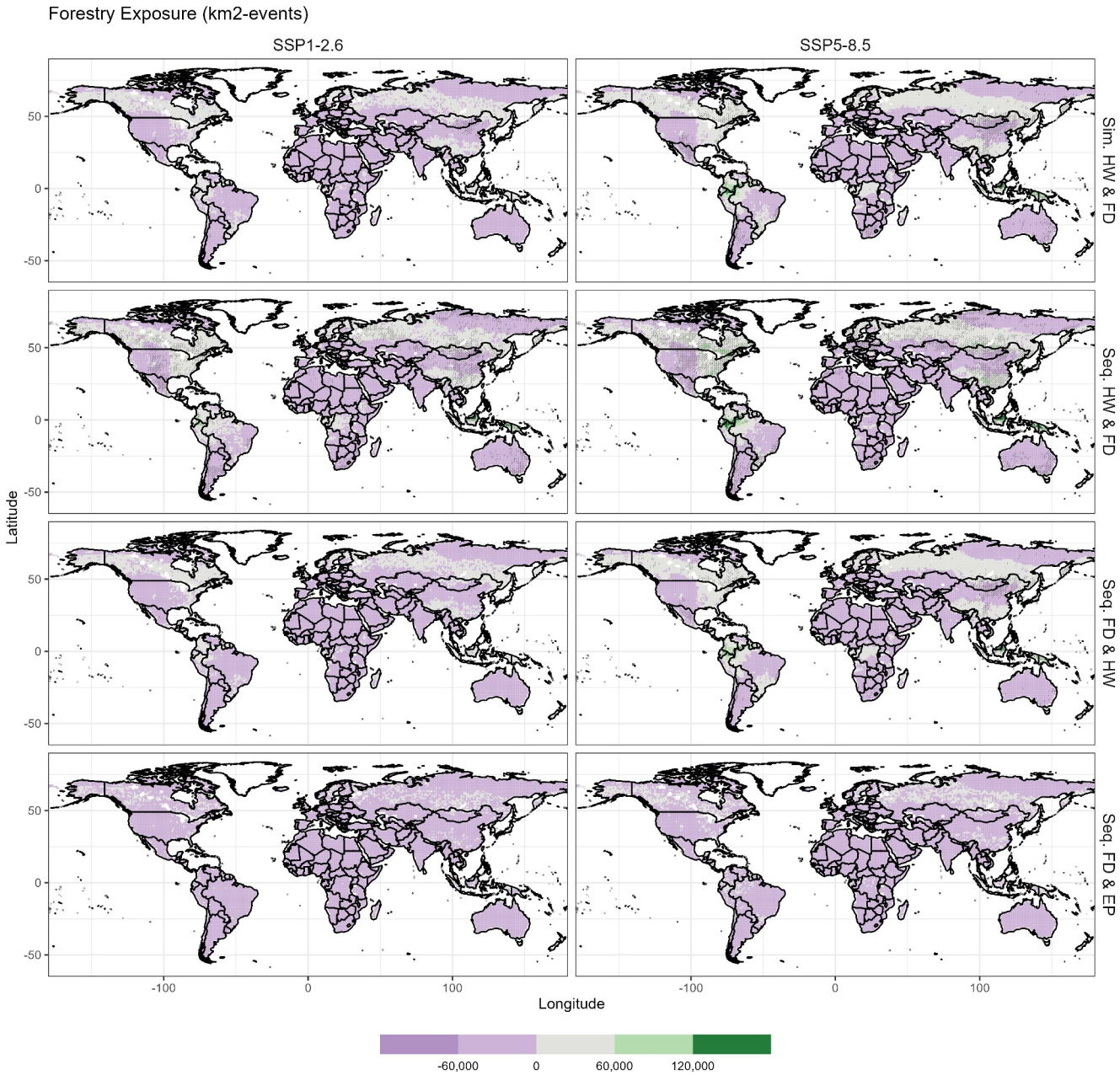

Figure 10. Change in forest land area exposed to simultaneous heatwave and flash drought (Sim. HW and FD), sequential heatwaves followed by flash droughts (Seq. HW and FD), sequential flash droughts followed by heatwaves (Seq. FD and HW), and sequential flash droughts followed by extreme precipitation (Seq. FD and EP) during early-, mid-, and late-century under SSP1-2.6 (left column) and SSP5-8.5 (right column) compared to historical. High model agreement areas are hashed.

Historically, the forest area exposed to simultaneous heatwave and flash drought events ranges from 10 to 530 km^2-event with an average exposure of 170 km^2-event across the regions (Figure S5 in Supporting Information S1). The amount of forest area exposure increase is higher in the late-century SSP5-8.5 scenario with an average additional exposure of 5,100 km^2-event late-century (Figure 8) and an average additional exposure of 680 km^2-event in the SSP1-2.6 scenario (Figure 7). South America has the highest increase in exposure of additional 14,000 km^2-event and 12,000 km^2-event by late-century in the SSP5-8.5 and SSP1-2.6 scenarios, respectively. The next highest increase in forest area exposure is the Oceania region for the SSP5-8.5 scenario. By late-century, forest exposure is expected to increase to 9,500 km^2-event. Scenario SSP1-2.6 projects smaller increases in forest exposure of 1,000 km^2-event on par with the exposure projected in North America for the same

period (1,200 km^2-event). Africa, China, Europe, and India are projected to have smaller increases (60–600 km^2-event) in additional exposure due to simultaneous heatwaves and flash drought events by late-century for the SSP1-2.6 scenario.

Sequential heatwaves and flash drought compound events have the highest regional historical forest exposure of 7,200 km^2-event (Figure S5 in Supporting Information S1). China, North America, Oceania, and South America have a projected increase in additional forest area exposure greater than 10,000 km^2-event (Figure 8) and 7,000 km^2-event (Figure 7) in the SSP5-8.5 and SSP1-2.6 scenarios. Europe has a smaller additional increase in exposure, 3,700 km^2-event, for late-century SSP5-8.5. Between the scenarios, Africa shows a decrease of 800 km^2-event in exposure when SSP5-8.5 is considered compared to the historical while SSP1-2.6 late-century shows an increase in exposure of 700 km^2-event. European and North American SSP1-2.6 projections show decreases in additional exposure from mid- to late-century.

For the historical reference period, forest area exposure for the selected regions is 90 km^2-event for sequential flash drought and heat wave events (Figure S5 in Supporting Information S1). This average is largely driven by the historical exposure of the North American and Indian regions (340 km^2-event and 90 km^2-event). The most considerable increased change by the SSP5-8.5 scenario late-century is projected in the South America region (12,000 km^2-event), followed by the Oceania region (8,200 km^2-event), North America, and China with similar increases (4,700 km^2-event and 3,000 km^2-event). The smallest increase projected in Europe (200 km^2-event) aligns with the small increases in sequential flash droughts, small increases in forest area, and weak model agreement. The SSP1-2.6 scenario forestry exposure is all under 1,000 km^2-event.

Sequential flash droughts and extreme precipitation have the smallest historical exposure, with an average of 30 km^2-event among the regions (Figure S5 in Supporting Information S1). For both scenarios, the increase in forest area exposure is very small, ranging from 5 to 200 km^2-event in the SSP5-8.5 scenario and 0–30 km^2-event in the SSP1-2.6 scenario. Sequential flash droughts and extreme precipitation have the least model agreement when calculating the projected change in the compound event and event exposure, which may have contributed to small exposure changes overall.

4. Discussion

In this study, we analyzed compound climate extremes: heatwave, extreme precipitation, and flash drought in the context of climate change using eight different CMIP6 models under two scenarios, SSP5-8.5 and SSP1-2.6. We find an average global increase of 8 and 4 heatwave events per year by late-century in the SSP5-8.5 and SSP1-2.6 scenarios, respectively. Extreme precipitation occurrences increases the most late-century to a global average of three events per year under SSP5-8.5 and only marginally under the SSP1-2.6 scenario. Flash drought occurrences are most substantial in the late-century SSP5-8.5 scenario; spatial patterns of change direction are largely inconsistent, with large deviations amounting to little change in global occurrence. Compound events derived from flash droughts have the most consistent land areas when heatwaves are followed by flash droughts, having the largest increases in the Oceania region with 21 events. China, North America, and South America experienced increases in sequential heatwaves and flash drought. Minor increases in simultaneous heatwave-flash drought events and sequential flash drought-heatwave events occur globally. Sequential flash drought and extreme precipitation events had the smallest increases in compound events, which transferred to the smallest population, agriculture, and forest exposure. The SSP5-8.5 scenario sequential heatwave-flash drought results in an additional exposure of 2.5 million person-events by late-century in China, Europe, North America, and the Oceania regions. The compound event also exposes agriculture areas (over 5,000 km^2-events) in China, Europe, North America, Oceania, and South America while simultaneously exposing an additional 75,000 km^2-events of forest in the Oceania region. This study provided assessments of compound extreme events and the exposure of different regions and sectors to these events, which could be potentially useful for policy and decision-makers to further understand climate risks and make adaption and mitigation strategies targeted on regions showing the most intense compound extreme events and exposures.

This research is distinct from previous studies in several aspects. First, we focus on daily calculations of compound events, which allows the inclusion of flash drought calculated from soil moisture besides extreme precipitation and heat waves. Past studies have largely focused on drought occurrences at a weekly or monthly scale, which may underestimate the impacts and severity of compound extreme events. Using a daily calculation for compound events allows further investigation into the severity and duration of the compound extreme events.

Second, we define dry and drought occurrences using soil moisture; in contrast to previous analysis of compound climate events, Das et al. (2022), and Weber et al. (2020) among others, define drought using a meteorological precipitation definition. Defining drought occurrences using soil moisture may lead to more impactful results because of the strong land-atmosphere feedback loops (Seneviratne et al., 2010). Defining drought using a deficit of precipitation fails to capture the anticipated changes in radiation, wind speed, and temperature, which affect evapotranspiration, impacting soil moisture content and water availability in ecosystems (Seneviratne et al., 2010). Third, we incorporate global exposure for populations, agriculture, and forest land areas. While population exposure for simultaneous hot-drought events has been well-researched (Li et al., 2023; W. Liu et al., 2021; Yin et al., 2023), we incorporate sequential versions of hot-drought and find that sequential heatwave and flash drought events to be more impactful. This is also true of global agricultural lands (X. Wu et al., 2021). However, we include exposure to forest lands from compound extreme events. The inclusion of forest lands is crucial for understanding the vulnerability of the carbon cycle and determining if forest will sequester carbon or release carbon (Anderegg et al., 2020) through tree mortality and wildfires.

Similar to Kong et al. (2020), Z. Liu et al. (2017), and Perkins-Kirkpatrick and Gibson (2017) we find an increase in extreme climate events related to heatwaves regionally and globally; the high increases in heatwaves near the equatorial region are also present in Perkins-Kirkpatrick and Gibson (2017) and Z. Liu et al. (2017). Like Tabari (2020), we also note an increase in global extreme precipitation events in central Africa; however, our results do not agree with the changes in the high latitudes. Christian et al. (2023) calculate flash drought in the future. Our results show similar spatial patterns of increase in the northern latitudes across Europe into Russia and Canada. While also showing decreases in portions of the African content. However, the change in flash droughts is not consistent in central South America (near Brazil), with Christian et al. (2023) showing increases in flash drought events and our results hinting at decreases in events. Both Christian et al. (2023) and our results have limited model agreement, leading to large uncertainties, and used different methods of flash drought calculation.

Within each sector (population, agriculture, and forest), different regions are exposed more than others. For projected population exposure, two regions, China and India, repeatedly have the highest exposure to sequential heatwaves and flash droughts, simultaneous heatwaves and flash droughts, and sequential flash droughts and heatwaves (Figures 7 and 8). When just sequential heatwaves and flash droughts are considered, Africa, Europe, and North America also have the highest exposure, with over 1 million person-events when SSP5-8.5 is considered (Figure 8). These findings that Europe, China, India, and North America when considered as a region support the findings from Li et al. (2023), W. Liu et al. (2021), Ullah et al. (2023), Weber et al. (2020), S. Wu et al. (2021), and Yin et al. (2023) that portions of these regions will see the highest population exposure to heatwaves and concurrent heatwaves and drought events. In the global studies, portions of western and central Africa show increases in population exposure. Figure 6 confirms that there is an increase in population exposure to compound events derived from heatwaves and flash droughts. Analysis combining Figures 5 and 6 suggests that urban centers with high populations will experience the highest increases in exposure. Increased exposure in these areas will put an added strain on infrastructure and increase mortality to sequential heatwave and drought-related compound events, prolonging impacts from heatwaves.

When sequential heatwaves and flash droughts are considered, mid-century population exposure for the China and India regions is the highest for both scenarios. This is likely due to projected population changes for each scenario. Population for China and other regions, including portions of Europe, North America, and South America, are expected to peak mid-century and decline to varying degrees by late-century (Jones & O'Neill, 2016). The population exposure, especially in China, may be underestimated due to fertility policies (Huang et al., 2019) that were enacted after the SSP population data set.

The exposure to agricultural lands experiencing projected changes in exposure varied across regions and compound event types. Overall, there appeared to be little increase in the projected changes of agricultural exposure to compound events (Figure 9) due to the decreases in agricultural lands (Figure 5). However, several breadbasket regions have a projected increase in exposure to compound events derived from combinations of simultaneous and sequential heatwave and flash drought exposure greater than 4,000 km^2-event by the late century when SSP5-8.5 is considered. These regions include China, Europe, India, North America, and South America. Increases in these regions of agriculture exposed to concurrent hot-dry events have occurred in the recent historical past (Lesk & Anderson, 2021) and support projected global increases noted by X. Wu et al. (2021). These regions are major

production areas for at least one of the following crops: maize, rice, soy, and wheat. Schillerberg and Tian (2023) note that the largest synchronized crop failure events in 2002 and 2012 occur when hot and dry events simultaneously occur throughout the growing season. Increases in occurrences in compound events, especially sequential heatwaves and flash drought events, can not only increase agriculture land exposure but also increase crop failure occurrences, highlighting the vulnerability of these systems and global food security. Additionally, adaption strategies relying on increasing irrigation may put an added strain on regional water supplies (Rosa, 2022). Adaption and mitigation strategies should consider the increase in sequential heatwave and drought events to promote new regional agricultural technologies, practices, crop types, and cultivars better suited to these projected increases.

Forest showed increases in exposure depending on regions and compound events. The largest increase in exposure occurred for sequential heatwave and flash drought, with several regions including China, North America, Oceania, and South America, each having increases of exposure greater than 10,000 km^2-event projected under the SSP5-8.5 scenario. Touma et al. (2022) highlighted an increase in fire weather conditions in the western United States; we confirm an increase in sequential heatwaves and flash droughts, which may contribute to fire weather conditions. Figure 10 displays large swaths of decreases in forest exposure this is partially due to projected decreases in land use devoted to forest (Figure 5) for both scenarios. Decreases in forest exposure late-century may also be due to declining forest health due to increases in extreme events and longer establishment and maturity periods needed (Aleixo et al., 2019). Forest land exposure to sequential heatwaves and droughts, which results in increases in China, North America, Oceania, and South America, has implications for carbon sequestration and storage, biodiversity, and wildfire events (Anderegg et al., 2020; Asbeck et al., 2021; Touma et al., 2022). Repeated exposure to compound events can increase tree and vegetation stress, making the trees vulnerable to pests, increasing tree mortality, resulting in ghost forests, and potentially increasing wildfire susceptibility.

We find that sequential heatwave and flash drought events have more model agreement, simultaneous heatwave-flash drought and sequential flash drought and heatwave have less agreement, and sequential flash drought and extreme precipitation have the least model agreement and least projected increases in occurrences. In Figures 1 and 2, we see a large uncertainty among the models of the flash drought trends, which may stem from the flash drought calculation. In the case of sequential heatwave-flash drought being more prominent, this may result from flash droughts being instigated by the heatwaves due to increases in evaporative demand (Hoffmann et al., 2021), and more likely with increasing temperatures. When flash droughts lead to heatwaves, the flash drought would have to be instigated by abnormally low precipitation. Sequential flash drought and extreme precipitation present the smallest change in compound events. This is likely due to the large uncertainty associated with flash droughts and extreme precipitation. This finding is on par with He and Sheffield (2020), who only find 5.9%–7.6% of global land surface experiences drought-heavy precipitation swings at the seasonal scale.

Despite the best efforts, this study has several caveats that need to be addressed in future studies. Flash drought is still a phenomenon that is being researched, and there is currently no consensus on flash drought definition (Christian et al., 2024). Therefore, we chose to define flash drought using a definition that has been used for flash drought analysis in CMIP climate models (Hoffmann et al., 2021), which required minimal variables and was calculatable using available model data. However, the occurrence of flash drought is influenced by the modeled soil moisture, which shows great uncertainties in climate model simulations. Another uncertainty is that we were limited to surface soil moisture, which is more variable than root zone soil column. In addition, we also acknowledge that our analysis is based on $1° \times 1°$ resolution data, which shows uncertainties and cannot capture the detailed variability of compound events and exposure with a grid cell. However, these results will still provide a starting point for stakeholders and decision-makers and where future research efforts with more accurate, finer-resolution models and data for exposure should be devoted.

Data Availability Statement

All climate data is available using one of the CMIP6 access nodes (i.e., https://esgf-node.ipsl.upmc.fr/search/cmip6-ipsl/); models used in this study are cited in the text. All analysis was performed using CDO version 2.0.4 and R version 4.2.2. The data generated from this study are available in Schillerberg and Tian (2024).

Acknowledgments
This work is supported in part by the NSF Research Traineeship Program (DGE-1922687), the NSF CAREER Award (EAR-2144293), and the Hatch program of the USDA National Institute of Food and Agriculture (NIFA) (Accession No. 1012578). We would like to acknowledge high-performance computing support provided by the Auburn University Easley Cluster.

References

AghaKouchak, A., Cheng, L., Mazdiyasni, O., & Farahmand, A. (2014). Global warming and changes in risk of concurrent climate extremes: Insights from the 2014 California drought. *Geophysical Research Letters*, *41*(24), 8847–8852. https://doi.org/10.1002/2014GL062308

Aleixo, I., Norris, D., Hemerik, L., Barbosa, A., Prata, E., Costa, F., & Poorter, L. (2019). Amazonian rainforest tree mortality driven by climate and functional traits. *Nature Climate Change*, *9*(5), 384–388. https://doi.org/10.1038/s41558-019-0458-0

Alexandrov, V. A., & Hoogenboom, G. (2000). Vulnerability and adaptation assessments of agricultural crops under climate change in the Southeastern USA. *Theoretical and Applied Climatology*, *67*(1–2), 45–63. https://doi.org/10.1007/s007040070015

Anderegg, W. R. L., Trugman, A. T., Badgley, G., Anderson, C. M., Bartuska, A., Ciais, P., et al. (2020). Climate-driven risks to the climate mitigation potential of forests. *Science*, *368*(6497), eaaz7005. https://doi.org/10.1126/science.aaz7005

Asbeck, T., Sabatini, F., Augustynczik, A. L. D., Basile, M., Helbach, J., Jonker, M., et al. (2021). Biodiversity response to forest management intensity, carbon stocks and net primary production in temperate montane forests. *Scientific Reports*, *11*(1), 1–11. https://doi.org/10.1038/s41598-020-80499-4

Ashley, S. T., & Ashley, W. S. (2008). Flood fatalities in the United States. *Journal of Applied Meteorology and Climatology*, *47*(3), 805–818. https://doi.org/10.1175/2007JAMC1611.1

Asseng, S., Ewert, F., Martre, P., Rötter, R. P., Lobell, D. B., Cammarano, D., et al. (2015). Rising temperatures reduce global wheat production. *Nature Climate Change*, *5*(2), 143–147. https://doi.org/10.1038/nclimate2470

Center for International Earth Science Information Network - CIESIN - Columbia University. (2011). *Foresight Project on Migration and Global Environmental Change, Report MR4: Estimating Net Migration by Ecosystem and by Decade, 1970–2010*. UK Government Foresight.

Center for International Earth Science Information Network - CIESIN - Columbia University. (2017). *Global Population Count Grid Time Series Estimates*. NASA Socioeconomic Data and Applications Center (SEDAC). https://doi.org/10.7927/H4CC0XNV

Charron, D. F., Thomas, M. K., Waltner-Toews, D., Aramini, J. J., Edge, T., Kent, R. A., et al. (2010). Vulnerability of waterborne diseases to climate change in Canada: A review. *Journal of Toxicology and Environmental Health, Part A*, *67*(20–22), 1667–1677. https://doi.org/10.1080/15287390490492313

Chen, H., & Sun, J. (2015). Changes in drought characteristics over China using the standardized precipitation evapotranspiration index. *Journal of Climate*, *28*(13), 5430–5447. https://doi.org/10.1175/JCLI-D-14-00707.1

Chitra-Tarak, R., Ruiz, L., Dattaraja, H. S., Mohan Kumar, M. S., Riotte, J., Suresh, H. S., et al. (2018). The roots of the drought: Hydrology and water uptake strategies mediate forest-wide demographic response to precipitation. *Journal of Ecology*, *106*(4), 1495–1507. https://doi.org/10.1111/1365-2745.12925

Christian, J. I., Basara, J. B., Hunt, E. D., Otkin, J. A., & Xiao, X. (2020). Flash drought development and cascading impacts associated with the 2010 Russian heatwave. *Environmental Research Letters*, *15*(9), 094078. https://doi.org/10.1088/1748-9326/AB9FAF

Christian, J. I., Hobbins, M., Hoell, A., Otkin, J. A., Ford, T. W., Cravens, A. E., et al. (2024). Flash drought: A state of the science review. *Wiley Interdisciplinary Reviews: Water*, *11*(3), e1714. https://doi.org/10.1002/WAT2.1714

Christian, J. I., Martin, E. R., Basara, J. B., Furtado, J. C., Otkin, J. A., Lowman, L. E. L., et al. (2023). Global projections of flash drought show increased risk in a warming climate. *Communications Earth & Environment*, *4*(1), 1–10. https://doi.org/10.1038/s43247-023-00826-1

Das, J., Manikanta, V., & Umamahesh, N. V. (2022). Population exposure to compound extreme events in India under different emission and population scenarios. *Science of the Total Environment*, *806*, 150424. https://doi.org/10.1016/j.scitotenv.2021.150424

De Sherbinin, A., Levy, M., Adamo, S., MacManus, K., Yetman, G., Mara, V., et al. (2012). Migration and risk: Net migration in marginal ecosystems and hazardous areas. *Environmental Research Letters*, *7*(4), 045602. https://doi.org/10.1088/1748-9326/7/4/045602

Eyring, V., Bony, S., Meehl, G. A., Senior, C. A., Stevens, B., Stouffer, R. J., & Taylor, K. E. (2016). Overview of the Coupled Model Intercomparison Project Phase 6 (CMIP6) experimental design and organization. *Geoscientific Model Development*, *9*(5), 1937–1958. https://doi.org/10.5194/gmd-9-1937-2016

Feng, S., Wu, X., Hao, Z., Hao, Y., Zhang, X., & Hao, F. (2020). A database for characteristics and variations of global compound dry and hot events. *Weather and Climate Extremes*, *30*, 100299. https://doi.org/10.1016/j.wace.2020.100299

Fischer, E. M., & Knutti, R. (2012). Robust projections of combined humidity and temperature extremes. *Nature Climate Change*, *3*(2), 126–130. https://doi.org/10.1038/nclimate1682

Ford, T. W., & Labosier, C. F. (2017). Meteorological conditions associated with the onset of flash drought in the Eastern United States. *Agricultural and Forest Meteorology*, *247*, 414–423. https://doi.org/10.1016/J.AGRFORMET.2017.08.031

Garry, F. K., Bernie, D. J., Davie, J. C. S., & Pope, E. C. D. (2021). Future climate risk to UK agriculture from compound events. *Climate Risk Management*, *32*, 100282. https://doi.org/10.1016/J.CRM.2021.100282

Gasparrini, A., Guo, Y., Hashizume, M., Lavigne, E., Zanobetti, A., Schwartz, J., et al. (2015). Mortality risk attributable to high and low ambient temperature: A multicountry observational study. *The Lancet*, *386*(9991), 369–375. https://doi.org/10.1016/S0140-6736(14)62114-0

Gerken, T., Bromley, G. T., Ruddell, B. L., Williams, S., & Stoy, P. C. (2018). Convective suppression before and during the United States Northern Great Plains flash drought of 2017. *Hydrology and Earth System Sciences*, *22*(8), 4155–4163. https://doi.org/10.5194/HESS-22-4155-2018

Haile, G. G., Tang, Q., Li, W., Liu, X., & Zhang, X. (2020). Drought: Progress in broadening its understanding. *Wiley Interdisciplinary Reviews: Water*, *7*(2), e1407. https://doi.org/10.1002/WAT2.1407

He, X., & Sheffield, J. (2020). Lagged compound occurrence of droughts and pluvials globally over the past seven decades. *Geophysical Research Letters*, *47*(14). https://doi.org/10.1029/2020GL087924

Hersbach, H., Bell, B., Berrisford, P., Biavati, G., Horányi, A., Muñoz Sabater, J., et al. (2023). *ERA5 hourly data on single levels from 1940 to present*. Copernicus Climate Data Store. https://doi.org/10.24381/cds.adbb2d47

Hoffmann, D., Gallant, A. J. E., & Hobbins, M. (2021). Flash drought in CMIP5 models. *Journal of Hydrometeorology*, *22*(6), 1439–1454. https://doi.org/10.1175/JHM-D-20-0262.1

Huang, J., Qin, D., Jiang, T., Wang, Y., Feng, Z., Zhai, J., et al. (2019). Effect of fertility policy changes on the population structure and economy of China: From the perspective of the shared socioeconomic pathways. *Earth's Future*, *7*(3), 250–265. https://doi.org/10.1029/2018EF000964

Hurtt, G. C., Chini, L., Sahajpal, R., Frolking, S., Bodirsky, B. L., Calvin, K., et al. (2020). Harmonization of global land use change and management for the period 850–2100 (LUH2) for CMIP6. *Geoscientific Model Development*, *13*(11), 5425–5464. https://doi.org/10.5194/GMD-13-5425-2020

Jones, B., & O'Neil, B. C. (2020). *Global one-eighth degree population base year and projection grids based on the shared socioeconomic pathways*. NASA Socioeconomic Data and Applications Center (SEDAC). https://doi.org/10.7927/m30p-j498

Jones, B., & O'Neill, B. C. (2016). Spatially explicit global population scenarios consistent with the Shared Socioeconomic Pathways. *Environmental Research Letters*, *11*(8), 084003. https://doi.org/10.1088/1748-9326/11/8/084003

Jones, B., O'Neill, B. C., Mcdaniel, L., Mcginnis, S., Mearns, L. O., & Tebaldi, C. (2015). Future population exposure to US heat extremes. *Nature Climate Change*, *5*(7), 652–655. https://doi.org/10.1038/nclimate2631
Karney, C. F. F. (2013). Algorithms for geodesics. *Journal of Geodesy*, *87*(1), 43–55. https://doi.org/10.1007/S00190-012-0578-Z/METRICS
Keellings, D., & Waylen, P. (2014). Increased risk of heat waves in Florida: Characterizing changes in bivariate heat wave risk using extreme value analysis. *Applied Geography*, *46*, 90–97. https://doi.org/10.1016/J.APGEOG.2013.11.008
Kong, Q., Guerreiro, S. B., Blenkinsop, S., Li, X. F., & Fowler, H. J. (2020). Increases in summertime concurrent drought and heatwave in Eastern China. *Weather and Climate Extremes*, *28*, 100242. https://doi.org/10.1016/J.WACE.2019.100242
Krishnamurthy, R. P. K., Fisher, J. B., Choularton, R. J., & Kareiva, P. M. (2022). Anticipating drought-related food security changes. *Nature Sustainability*, *2022*, 1–9. https://doi.org/10.1038/s41893-022-00962-0
Lan, L., Cui, G., Yang, C., Wang, J., Sui, C., Xu, G., et al. (2012). Increased mortality during the 2010 heat wave in Harbin, China. *EcoHealth*, *9*(3), 310–314. https://doi.org/10.1007/S10393-012-0790-6/TABLES/2
Lesk, C., & Anderson, W. (2021). Decadal variability modulates trends in concurrent heat and drought over global croplands. *Environmental Research Letters*, *16*(5), 055024. https://doi.org/10.1088/1748-9326/ABEB35
Li, B., Liu, K., Wang, M., Wang, Q., He, Q., & Li, C. (2023). Future global population exposure to record-breaking climate extremes. *Earth's Future*, *11*(11), e2023EF003786. https://doi.org/10.1029/2023EF003786
Liu, B., Zhang, D., Zhang, H., Asseng, S., Yin, T., Qiu, X., et al. (2021). Separating the impacts of heat stress events from rising mean temperatures on winter wheat yield of China. *Environmental Research Letters*, *16*(12), 124035. https://doi.org/10.1088/1748-9326/AC3870
Liu, W., Sun, F., Feng, Y., Li, C., Chen, J., Sang, Y. F., & Zhang, Q. (2021). Increasing population exposure to global warm-season concurrent dry and hot extremes under different warming levels. *Environmental Research Letters*, *16*(9), 094002. https://doi.org/10.1088/1748-9326/ac188f
Liu, Z., Anderson, B., Yan, K., Dong, W., Liao, H., & Shi, P. (2017). Global and regional changes in exposure to extreme heat and the relative contributions of climate and population change. *Scientific Reports*, *7*(1), 1–9. https://doi.org/10.1038/srep43909
Ma, F., & Yuan, X. (2021). Impact of climate and population changes on the increasing exposure to summertime compound hot extremes. *Science of the Total Environment*, *772*, 145004. https://doi.org/10.1016/j.scitotenv.2021.145004
Mangani, R., Tesfamariam, E. H., Bellocchi, G., & Hassen, A. (2018). Growth, development, leaf gaseous exchange, and grain yield response of maize cultivars to drought and flooding stress. *Sustainability*, *10*(10), 3492. https://doi.org/10.3390/su10103492
Mishra, V., Mukherjee, S., Kumar, R., & Stone, D. A. (2017). Heat wave exposure in India in current, 1.5°C, and 2.0°C worlds. *Environmental Research Letters*, *12*(12), 124012. https://doi.org/10.1088/1748-9326/AA9388
Mukherjee, S., & Mishra, A. K. (2020). Increase in compound drought and heatwaves in a warming World. *Geophysical Research Letters*, *48*(1), e2020GL090617. https://doi.org/10.1029/2020GL090617
Nguyen, H., Wheeler, M. C., Otkin, J. A., Cowan, T., Frost, A., & Stone, R. (2019). Using the evaporative stress index to monitor flash drought in Australia. *Environmental Research Letters*, *14*(6), 064016. https://doi.org/10.1088/1748-9326/AB2103
NOAA National Centers for Environmental Information (NCEI). (2024). U.S. Billion-Dollar Weather and Climate Disasters. https://doi.org/10.25921/stkw-7w73
O'Neill, B. C., Kriegler, E., Riahi, K., Ebi, K. L., Hallegatte, S., Carter, T. R., et al. (2014). A new scenario framework for climate change research: The concept of shared socioeconomic pathways. *Climatic Change*, *122*(3), 387–400. https://doi.org/10.1007/S10584-013-0905-2/TABLES/2
Otkin, J. A., Anderson, M. C., Hain, C., Svoboda, M., Johnson, D., Mueller, R., et al. (2016). Assessing the evolution of soil moisture and vegetation conditions during the 2012 United States flash drought. *Agricultural and Forest Meteorology*, *218–219*, 230–242. https://doi.org/10.1016/J.AGRFORMET.2015.12.065
Otkin, J. A., Svoboda, M., Hunt, E. D., Ford, T. W., Anderson, M. C., Hain, C., & Basara, J. B. (2018). Flash droughts: A review and assessment of the challenges imposed by rapid-onset droughts in the United States. *Bulletin of the American Meteorological Society*, *99*(5), 911–919. https://doi.org/10.1175/BAMS-D-17-0149.1
Peltonen-Sainio, P., Jauhiainen, L., & Hakala, K. (2011). Crop responses to temperature and precipitation according to long-term multi-location trials at high-latitude conditions. *Journal of Agricultural Science*, *149*(1), 49–62. https://doi.org/10.1017/S0021859610000791
Perkins-Kirkpatrick, S. E., & Gibson, P. B. (2017). Changes in regional heatwave characteristics as a function of increasing global temperature. *Scientific Reports*, *7*(1), 1–12. https://doi.org/10.1038/s41598-017-12520-2
Popp, A., Calvin, K., Fujimori, S., Havlik, P., Humpenöder, F., Stehfest, E., et al. (2017). Land-use futures in the shared socio-economic pathways. *Global Environmental Change*, *42*, 331–345. https://doi.org/10.1016/J.GLOENVCHA.2016.10.002
Qiu, J., Shen, Z., Leng, G., & Wei, G. (2021). Synergistic effect of drought and rainfall events of different patterns on watershed systems. *Scientific Reports 2021*, *11*(1), 1–18. https://doi.org/10.1038/s41598-021-97574-z
Robinson, P. J. (2001). On the definition of a heat wave. *Journal of Applied Meteorology*, *40*(4), 762–775. https://doi.org/10.1175/1520-0450(2001)040<0762:OTDOAH>2.0.CO;2
Rosa, L. (2022). Adapting agriculture to climate change via sustainable irrigation: Biophysical potentials and feedbacks. *Environmental Research Letters*, *17*(6), 063008. https://doi.org/10.1088/1748-9326/AC7408
Ruosteenoja, K., Markkanen, T., Venäläinen, A., Räisänen, P., & Peltola, H. (2018). Seasonal soil moisture and drought occurrence in Europe in CMIP5 projections for the 21st century. *Climate Dynamics*, *50*(3–4), 1177–1192. https://doi.org/10.1007/S00382-017-3671-4/FIGURES/9
Schillerberg, T., & Tian, D. (2023). Changes in crop failures and their predictions with agroclimatic conditions: Analysis based on earth observations and machine learning over global croplands. *Agricultural and Forest Meteorology*, *340*, 109620. https://doi.org/10.1016/J.AGRFORMET.2023.109620
Schillerberg, T., & Tian, D. (2024). Global assessment of compound climate extremes and exposures of population, agriculture, and forest lands under two climate scenarios. [Dataset]. *OSF*. https://doi.org/10.17605/OSF.IO/6SDGQ
Seneviratne, S. I., Corti, T., Davin, E. L., Hirschi, M., Jaeger, E. B., Lehner, I., et al. (2010). Investigating soil moisture–climate interactions in a changing climate: A review. *Earth-Science Reviews*, *99*(3–4), 125–161. https://doi.org/10.1016/J.EARSCIREV.2010.02.004
Seneviratne, S. I., Zhang, X., Adnan, M., Badi, W., Dereczynski, C., Di Luca, A., et al. (2021). Weather and climate extreme events in a changing climate (Chapter 11). In V. Masson-Delmotte, P. Zhai, A. Pirani, S. L. Connors, C. Pean, S. Berger, et al. (Eds.), *IPCC 2021: Climate Change 2021: The Physical Science Basis. Contribution of Working Group I to the Sixth Assessment Report of the Intergovernmental Panel on Climate Change* (pp. 1513–1766). Cambridge University Press. https://doi.org/10.1017/9781009157896.013
Svoboda, M., LeComte, D., Hayes, M., Heim, R., Gleason, K., Angel, J., et al. (2002). The drought monitor. *Bulletin of the American Meteorological Society*, *83*(8), 1181–1190. https://doi.org/10.1175/1520-0477(2002)083<1181:TDM>2.3.CO;2
Tabari, H. (2020). Climate change impact on flood and extreme precipitation increases with water availability. *Scientific Reports*, *10*(1), 1–10. https://doi.org/10.1038/s41598-020-70816-2
Takle, E. S., & Gutowski, W. J. (2020). Iowa's agriculture is losing its Goldilocks climate. *Physics Today*, *73*(2), 26–33. https://doi.org/10.1063/PT.3.4407

Touma, D., Stevenson, S., Swain, D. L., Singh, D., Kalashnikov, D. A., & Huang, X. (2022). Climate change increases risk of extreme rainfall following wildfire in the western United States. *Science Advances*, *8*(13), eabm0320. https://doi.org/10.1126/sciadv.abm0320
Ullah, I., Zeng, X. M., Mukherjee, S., Aadhar, S., Mishra, A. K., Syed, S., et al. (2023). Future amplification of multivariate risk of compound drought and heatwave events on South Asian population. *Earth's Future*, *11*(12), e2023EF003688. https://doi.org/10.1029/2023EF003688
Wang, C., Li, Z., Chen, Y., Ouyang, L., Li, Y., Sun, F., et al. (2023). Drought-heatwave compound events are stronger in drylands. *Weather and Climate Extremes*, *42*, 100632. https://doi.org/10.1016/J.WACE.2023.100632
Weber, T., Bowyer, P., Rechid, D., Pfeifer, S., Raffaele, F., Remedio, A. R., et al. (2020). Analysis of compound climate extremes and exposed population in Africa under two different emission scenarios. *Earth's Future*, *8*(9), 1–19. https://doi.org/10.1029/2019EF001473
Wolfe, D. W., DeGaetano, A. T., Peck, G. M., Carey, M., Ziska, L. H., Lea-Cox, J., et al. (2018). Unique challenges and opportunities for northeastern US crop production in a changing climate. *Climatic Change*, *146*(1–2), 231–245. https://doi.org/10.1007/s10584-017-2109-7
World Economic Forum. (2024). *The global risks report 2024*. World Economic Forum. Retrieved from https://www.weforum.org/publications/global-risks-report-2024/
Wu, S., Wang, P., Tong, X., Tian, H., Zhao, Y., & Luo, M. (2021). Urbanization-driven increases in summertime compound heat extremes across China. *Science of the Total Environment*, *799*, 149166. https://doi.org/10.1016/J.SCITOTENV.2021.149166
Wu, X., Hao, Z., Tang, Q., Singh, V. P., Zhang, X., & Hao, F. (2021). Projected increase in compound dry and hot events over global land areas. *International Journal of Climatology*, *41*(1), 393–403. https://doi.org/10.1002/joc.6626
Xu, Z., FitzGerald, G., Guo, Y., Jalaludin, B., & Tong, S. (2016). Impact of heatwave on mortality under different heatwave definitions: A systematic review and meta-analysis. *Environment International*, *89*(90), 193–203. https://doi.org/10.1016/j.envint.2016.02.007
Yin, J., Gentine, P., Slater, L., Gu, L., Pokhrel, Y., Hanasaki, N., et al. (2023). Future socio-ecosystem productivity threatened by compound drought–heatwave events. *Nature Sustainability*, *6*(3), 259–272. https://doi.org/10.1038/s41893-022-01024-1
Yuan, X., Wang, Y., Ji, P., Wu, P., Sheffield, J., & Otkin, J. A. (2023). A global transition to flash droughts under climate change. *Science*, *380*(6641), 187–191. https://doi.org/10.1126/science.abn6301
Zhang, M., & Yuan, X. (2020). Rapid reduction in ecosystem productivity caused by flash droughts based on decade-long FLUXNET observations. *Hydrology and Earth System Sciences*, *24*(11), 5579–5593. https://doi.org/10.5194/HESS-24-5579-2020
Zhang, Y., Hao, Z., Zhang, X., & Hao, F. (2022). Anthropogenically forced increases in compound dry and hot events at the global and continental scales. *Environmental Research Letters*, *17*(2), 024018. https://doi.org/10.1088/1748-9326/ac43e0
Zhou, S., Yu, B., & Zhang, Y. (2023). Global concurrent climate extremes exacerbated by anthropogenic climate change. *Science Advances*, *9*(10), eabo1638. https://doi.org/10.1126/sciadv.abo1638
Zscheischler, J., Martius, O., Westra, S., Bevacqua, E., Raymond, C., Horton, R. M., et al. (2020). A typology of compound weather and climate events. *Nature Reviews Earth and Environment*, *1*(7), 333–347. https://doi.org/10.1038/s43017-020-0060-z
Zscheischler, J., Westra, S., Van Den Hurk, B. J. J. M., Seneviratne, S. I., Ward, P. J., Pitman, A., et al. (2018). Future climate risk from compound events. *Nature Climate Change*, *8*(6), 469–477. https://doi.org/10.1038/s41558-018-0156-3

References From the Supporting Information

Bentsen, M., Oliviè, D. J. L., Seland, O., Toniazzo, T., Gjermundsen, A., Graff, L. S., et al. (2019a). *NCC NorESM2-MM model output prepared for CMIP6 CMIP historical*. Earth System Grid Federation. https://doi.org/10.22033/ESGF/CMIP6.8040
Bentsen, M., Oliviè, D. J. L., Seland, O., Toniazzo, T., Gjermundsen, A., Graff, L. S., et al. (2019b). *NCC NorESM2-MM model output prepared for CMIP6 ScenarioMIP ssp126*. Earth System Grid Federation. https://doi.org/10.22033/ESGF/CMIP6.8250
Bentsen, M., Oliviè, D. J. L., Seland, O., Toniazzo, T., Gjermundsen, A., Graff, L. S., et al. (2019c). *NCC NorESM2-MM model output prepared for CMIP6 ScenarioMIP ssp585*. Earth System Grid Federation. https://doi.org/10.22033/ESGF/CMIP6.8321
EC-Earth Consortium (EC-Earth). (2019a). *EC-Earth-Consortium EC-Earth3 model output prepared for CMIP6 CMIP historical*. Earth System Grid Federation. https://doi.org/10.22033/ESGF/CMIP6.4700
EC-Earth Consortium (EC-Earth). (2019b). *EC-Earth-Consortium EC-Earth3 model output prepared for CMIP6 ScenarioMIP ssp126*. Earth System Grid Federation. https://doi.org/10.22033/ESGF/CMIP6.4874
EC-Earth Consortium (EC-Earth). (2019c). *EC-Earth-Consortium EC-Earth3 model output prepared for CMIP6 ScenarioMIP ssp585*. Earth System Grid Federation. https://doi.org/10.22033/ESGF/CMIP6.4912
Fatolahzadeh Gheysari, A., Maghoul, P., Ojo, E. R., & Shalaby, A. (2024). Reliability of ERA5 and ERA5-Land reanalysis data in the Canadian Prairies. *Theoretical and Applied Climatology*, *155*(4), 3087–3098. https://doi.org/10.1007/s00704-023-04771-z
Gomis-Cebolla, J., Rattayova, V., Salazar-Galán, S., & Francés, F. (2023). Evaluation of ERA5 and ERA5-Land reanalysis precipitation datasets over Spain (1951–2020). *Atmospheric Research*, *284*, 106606. https://doi.org/10.1016/j.atmosres.2023.106606
John, J. G., Blanton, C., McHugh, C., Radhakrishnan, A., Rand, K., Vahlenkamp, H., et al. (2018a). *NOAA-GFDL GFDL-ESM4 model output prepared for CMIP6 ScenarioMIP ssp126*. Earth System Grid Federation. https://doi.org/10.22033/ESGF/CMIP6.8684
John, J. G., Blanton, C., McHugh, C., Radhakrishnan, A., Rand, K., Vahlenkamp, H., et al. (2018b). *NOAA-GFDL GFDL-ESM4 model output prepared for CMIP6 ScenarioMIP ssp585*. Earth System Grid Federation. https://doi.org/10.22033/ESGF/CMIP6.8706
Jungclaus, J., Bittner, M., Wieners, K.-H., Wachsmann, F., Schupfner, M., Legutke, S., et al. (2019). *MPI-M MPI-ESM1.2-HR model output prepared for CMIP6 CMIP historical*. Earth System Grid Federation. https://doi.org/10.22033/ESGF/CMIP6.6594
Krasting, J. P., John, J. G., Blanton, C., McHugh, C., Nikonov, S., Radhakrishnan, A., et al. (2018). *NOAA-GFDL GFDL-ESM4 model output prepared for CMIP6 CMIP esm-hist*. Earth System Grid Federation. https://doi.org/10.22033/ESGF/CMIP6.8522
Lovato, T., Peano, D., & Butenschön, M. (2021a). *CMCC CMCC-ESM2 model output prepared for CMIP6 CMIP historical*. Earth System Grid Federation. https://doi.org/10.22033/ESGF/CMIP6.13195
Lovato, T., Peano, D., & Butenschön, M. (2021b). *CMCC CMCC-ESM2 model output prepared for CMIP6 ScenarioMIP ssp126*. Earth System Grid Federation. https://doi.org/10.22033/ESGF/CMIP6.13250
Lovato, T., Peano, D., & Butenschön, M. (2021c). *CMCC CMCC-ESM2 model output prepared for CMIP6 ScenarioMIP ssp585*. Earth System Grid Federation. https://doi.org/10.22033/ESGF/CMIP6.13259
Maraun, D., Shepherd, T. G., Widmann, M., Zappa, G., Walton, D., Gutiérrez, J. M., et al. (2017). Towards process-informed bias correction of climate change simulations. *Nature Climate Change*, *7*(11), 764–773. https://doi.org/10.1038/nclimate3418
Schupfner, M., Wieners, K.-H., Wachsmann, F., Steger, C., Bittner, M., Jungclaus, J., et al. (2019a). *DKRZ MPI-ESM1.2-HR model output prepared for CMIP6 ScenarioMIP ssp126*. Earth System Grid Federation. https://doi.org/10.22033/ESGF/CMIP6.4397
Schupfner, M., Wieners, K.-H., Wachsmann, F., Steger, C., Bittner, M., Jungclaus, J., et al. (2019b). *DKRZ MPI-ESM1.2-HR model output prepared for CMIP6 ScenarioMIP ssp585*. Earth System Grid Federation. https://doi.org/10.22033/ESGF/CMIP6.4403

Volodin, E., Mortikov, E., Gritsun, A., Lykossov, V., Galin, V., Diansky, N., et al. (2019a). *INM INM-CM4-8 model output prepared for CMIP6 CMIP historical*. Earth System Grid Federation. https://doi.org/10.22033/ESGF/CMIP6.5069

Volodin, E., Mortikov, E., Gritsun, A., Lykossov, V., Galin, V., Diansky, N., et al. (2019b). *INM INM-CM4-8 model output prepared for CMIP6 ScenarioMIP ssp126*. Earth System Grid Federation. https://doi.org/10.22033/ESGF/CMIP6.12325

Volodin, E., Mortikov, E., Gritsun, A., Lykossov, V., Galin, V., Diansky, N., et al. (2019c). *INM INM-CM4-8 model output prepared for CMIP6 ScenarioMIP ssp585*. Earth System Grid Federation. https://doi.org/10.22033/ESGF/CMIP6.12337

Volodin, E., Mortikov, E., Gritsun, A., Lykossov, V., Galin, V., Diansky, N., et al. (2019d). *INM INM-CM5-0 model output prepared for CMIP6 CMIP historical*. Earth System Grid Federation. https://doi.org/10.22033/ESGF/CMIP6.5070

Volodin, E., Mortikov, E., Gritsun, A., Lykossov, V., Galin, V., Diansky, N., et al. (2019e). *INM INM-CM5-0 model output prepared for CMIP6 ScenarioMIP ssp126*. Earth System Grid Federation. https://doi.org/10.22033/ESGF/CMIP6.12326

Volodin, E., Mortikov, E., Gritsun, A., Lykossov, V., Galin, V., Diansky, N., et al. (2019f). *INM INM-CM5-0 model output prepared for CMIP6 ScenarioMIP ssp585*. Earth System Grid Federation. https://doi.org/10.22033/ESGF/CMIP6.12338

Wilks, D. S. (2011). Statistical methods in the atmospheric sciences. In R. Dmowska, D. Hartmann, & H. T. Rossby (Eds.), *International Geophysics Series* (3rd ed., Vol. 100). Academic Press.

Yukimoto, S., Koshiro, T., Kawai, H., Oshima, N., Yoshida, K., Urakawa, S., et al. (2019a). *MRI MRI-ESM2.0 model output prepared for CMIP6 CMIP historical*. Earth System Grid Federation. https://doi.org/10.22033/ESGF/CMIP6.6842

Yukimoto, S., Koshiro, T., Kawai, H., Oshima, N., Yoshida, K., Urakawa, S., et al. (2019b). *MRI MRI-ESM2.0 model output prepared for CMIP6 ScenarioMIP ssp126*. Earth System Grid Federation. https://doi.org/10.22033/ESGF/CMIP6.6909

Yukimoto, S., Koshiro, T., Kawai, H., Oshima, N., Yoshida, K., Urakawa, S., et al. (2019c). *MRI MRI-ESM2.0 model output prepared for CMIP6 ScenarioMIP ssp585*. Earth System Grid Federation. https://doi.org/10.22033/ESGF/CMIP6.6929